A subaquatic moraine complex in overdeepened Lake Thun (Switzerland) unravelling the deglaciation history of the Aare Glacier

S.C. Fabbri[1*], M.W. Buechi[2], H. Horstmeyer[3], M. Hilbe[2], C. Hübscher[4], C. Schmelzbach[3], B. Weiss[4], F.S. Anselmetti[2]

[1] Institute of Geological Sciences, Baltzerstrasse 1+3, 3012 Bern, Switzerland

[2] Institute of Geological Sciences, Oeschger Centre of Climate Change Research, University of Bern, Baltzerstrasse 1+3, 3012 Bern, Switzerland

[3] Institute of Geophysics, Dept. of Earth Sciences, Sonneggstr. 5, ETH Zürich, CH-8092, Zürich, Switzerland

[4] Institute of Geophysics, Center for Earth System Research and Sustainability, University of Hamburg, Bundesstr. 55, D-20146 Hamburg, Germany

*Corresponding author

Keywords: Quaternary, Deglaciation, Western Europe, Aare Valley, Overdeepening, , Seismic Stratigraphy, Subaquatic Moraine Complex, Gemorphology(glacial)

Abstract

To investigate the history of the Aare Glacier and its overdeepened valley, a high-resolution multibeam bathymetric dataset and a 2D multi-channel reflection seismic dataset were acquired on perialpine Lake Thun (Switzerland). The overdeepened basin was formed by a combination of tectonically predefined weak zones and glacial erosion during several glacial cycles. In the deepest region of the basin, top of bedrock lies at ~200 m below sea level, implying more than 750 m of overdeepening with respect to the current fluvial base level (i.e. lake level). Seismic stratigraphic analysis reveals the evolution of the basin and indicates a subaquatic moraine complex marked by high-amplitude reflections below the outermost edge of a morphologically distinct platform in the southeastern part of the lake. This stack of seven subaquatic terminal moraine crests was created by a fluctuating, “quasi-stagnant” grounded Aare Glacier during its overall recessional phase. Single packages of overridden moraine crests are seismically distuinguishable, which show a transition downstream into prograding clinoforms with foresets at the ice-distal slope. The succession of subaquatic glacial sequences (foresets and adjacent bottomsets) represent one fifth of the entire sedimentary thickness.

Exact time constraints concerning the deglacial history of the Aare Glacier are very sparse. However, existing ^{10}Be exposure ages from the accumulation area of the Aare Glacier and radiocarbon ages from a Late-Glacial lake close to the outlet of Lake Thun indicate that the formation of the subaquatic moraine complex and the associated sedimentary infill must have occurred in less than 1,000 years, implying high sedimentation rates and rapid disintegration of the glacier.

These new data improve our comprehension of the landforms associated with the ice-contact zone in water, the facies architecture of the sub- to proglacial units, the related depositional processes, and thus the retreat mechanisms of the Aare Glacier.

1. Introduction

The evolution of the Quaternary landscape and the formation of Alpine valleys has been of scientific interest for generations of geologists over the last 200 years (e.g. Escher, 1820; Penck, 1905), seeking for explanations that elucidate the creation of perialpine lakes and overdeepened troughs (Bini et al., 1978; Finckh, 1978). In recent years, glacial overdeepenings attracted economic interest, since a majority of these troughs host aquifers with drinking water, and major engineering and tunneling projects across the Alps encountered unexpected challenges with the sedimentary infill and morphology of them (e.g. Lötschberg railway tunnel, Schlüchter, 1979). Furthermore, the Swiss nuclear waste disposal program aims at finding a safe repository for high-level nuclear waste that endures future glacial cycles, which requires an improved understanding of factors controlling glacio-fluvial erosion, overdeepening processes and glacial advances and retreat phases of the local Aare, Rhine and Rhone Glacier system (Preusser et al., 2010).

The important role of perialpine lakes for the unravelling of the (de-) glaciation history of the Alps was already recognized by Heim (1894) in Lake Lucerne (Switzerland). The detailed sedimentary archives of lakes serve as excellent trackers of glacial evolution. Moreover, morphological features, which are sometimes hard to identify on land, are perfectly preserved in lacustrine and marine environments, where erosional processes are strongly hampered. Examples of subaquatic glacial morphologies have been shown for example in the fjord basin of Lake Melville, southeast Labrador, Canada (Lønne and Syvitski, 1997), in Lago Fagnano, southern Patagonia (Waldmann et al., 2010), or in central Sweden, where a series of subaquatic end moraines is reported (Johnson et al., 2013).

The global Last Glacial Maximum (LGM, Mix et al., 2001; Clark et al., 2009; Hughes et al., 2013) does temporally fairly well coincide with the maximum reach out of Alpine piedmont glaciers into the northern foreland and the creation of the Italian amphitheatres in the south between 26 ka and 19 ka (Ivy-Ochs, 2015; Monegato et al., 2017, Fig. 1A). The maximum ice extent of the Rhone Glacier, was reached at or slightly before 24.0 ± 1.1 ka, as reported by Reber et al. (2014). They dated the abandonment of the Rhone Glacier's maximum position to 19.1 ± 1.5 ka, in response to an initial pre-Bølling deglacial phase, which is in good agreement with the onset of deglaciation of the Aare Glacier (Akcar et al., 2011). It seems that Alpine glaciers act very sensitively to slight snowline changes and therefore respond rapidly to temperature changes, collapsing faster during warming pulses (Ivy-Ochs et al., 2004).

The Quaternary landscape created by the Aare Glacier between Bern and the accumulation area at Grimselpass was first described by Penck and Brückner (1909). Beck (1920-1922) noticed that the complete excavation of sedimentary infill in an overdeepened valley during the Würmian glaciation is rather unlikely. The records from drilling sites at Meikirch NW of Bern (Welten, 1988) and at Thalgut (Schlüchter, 1989b, Fig. 1B) north of Thun serve as ideal Quaternary archives to support his claim. The latter reveals top of Molasse bedrock at 147 m depth below surface with at least three glacial cycles covering it (Schlüchter and Kelly, 2000). A basal glacial unit is followed by the lowermost lacustrine clays being indicative for the Holstein Interglacial associated with MIS 9 (Schlüchter, 1989b, 1989a). This implies that bedrock erosion to the current level occurred during the glaciation in MIS 10 or even earlier at Thalgut. The sequence is topped with a basal lodgment till deposited during LGM (Preusser and Schlüchter, 2004). At Meikirch, deposits of previous glacial cycles are preserved as well, and the last time bedrock experienced ice contact was during MIS 8 or earlier based on the re-interpretation of sediment logs, palynological correlation and luminescence dating (Preusser et al., 2005). Other drill holes within overdeepened basins revealed similar deposits of previous glacial cycles and showed their preservation potential over several glaciations (e.g. Salzach, Germany: (e.g Niederweningen, Switzerland: Anselmetti et al., 2010; Dehnert et al., 2012; Salzach, Austria/Germany: Fiebig et al., 2014; Lower Glatt Valley, Switzerland: Buechi et al., 2017).

In contrast to our fairly good understanding of the ice extent during LGM along the Alps (Fig. 1A), the deglaciation history of the LGM is still poorly constrained and mostly based on ice-marginal landforms, trimlines, striae, roches moutonnées, polished bedrock and erratic boulders (e.g. Jäckli, 1962; Schlüchter, 1988). More recent studies in the Upper Aare Valley incorporate surface exposure ages derived from in-situ produced cosmogenic nuclides such as ^{10}Be in boulders and bedrock (e.g. Ivy-Ochs and Kober, 2008; Akcar et al., 2011). Kelly et al. (2006) and Wirsig et al. (2016) reconstructed the retreat and stagnant episodes of the Aare Glacier during its recessional phase from the abandonment of its LGM position northeast of Bern to its accumulation area at Grimselpass using ^{10}Be. The rapid ice decay in the northern foreland (Schlüchter, 1988) hardly left any obvious moraines hinting at a stabilization of the ice front or a Late-Glacial readvance beyond the inner-Alpine regions (Kelly et al., 2006; Reitner et al., 2016). Ivy-Ochs et al. (2006) also notes that, despite detailed geologic mapping for more than 100 years, Gschnitz moraines (Kerschner et al., 1999) have not been found yet in major longitudinal valleys within the Alps.

Our extensive multi-channel reflection seismic survey combined with multibeam swath bathymetry on Lake Thun enable us to perform a detailed study of the bedrock topography and the sedimentary infill of its overdeepened basin, both containing several glacial features. We present the seismic stratigraphy displaying the detailed internal structure of a previously unknown large subaquatic moraine complex, including a model that gives a relative chronology of its build-up. Our findings shed new light on the understanding of the deglaciation history of the Aare valley, and will address some challenges associated with the often poorly constrained estimation of overdeepening in perialpine lakes.

1.1. Geological setting

Perialpine Lake Thun lies at the northern front of the Alpine nappes and is situated in the upper Aare valley between Interlaken and Bern (Fig. 1A). Its overdeepened basin is located within sedimentary Penninic and Helvetic thrust nappes and the Subalpine Molasse outcropping on the southwest, northeast and northern shores, respectively. The main part of the Lake Thun basin is elongated orthogonal to the general strike direction of the Alpine front (WSW-ENE).

During the Pleistocene glaciations, subglacial erosion formed overdeepenings and shaped the study area (Haeuselmann et al., 2007; Reber and Schlunegger, 2016). Ice thickness of the valley glacier may have varied between these different glaciations, but must have reached several hundred meters of ice (ice elevation at ~1200 m a.s.l at Thun and 3000 m a.s.l. at the accumulation area of the Aare Glacier) during the LGM (Bini et al., 2009). Prominent glacial landforms attributed to the last glacial period are limited to the southern shoreline of the lake (Fig. 1C), where a number of relatively continuous lateral moraine ridges run parallel to the lake axis. Furthermore, a drumlin field and ribbed moraines have been described in the area W of Thun (Beck, 1933; Fiore, 2007).

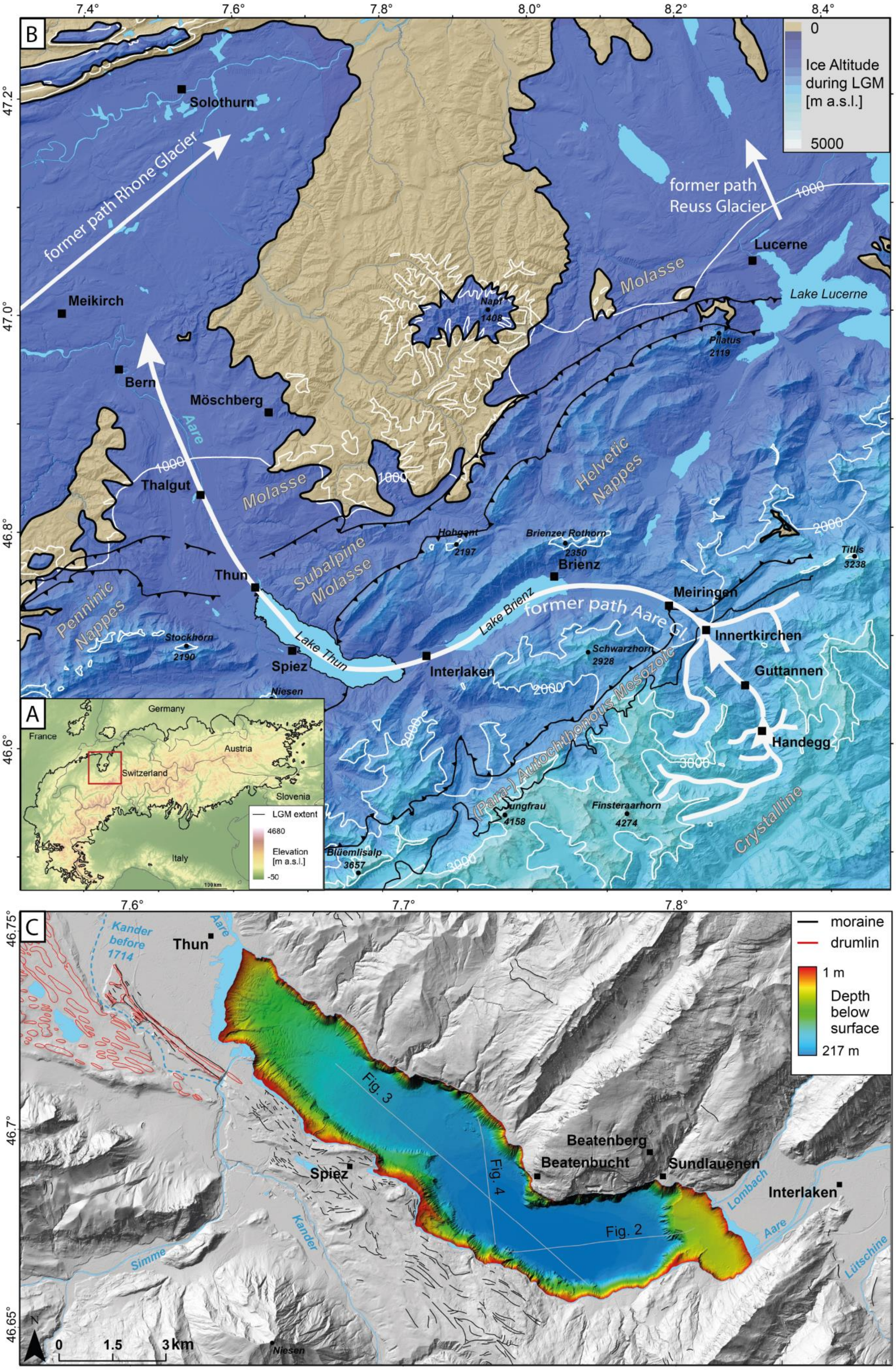

B
Ice Altitude during LGM [m a.s.l.]
0
5000
Solothurn
former path Rhone Glacier
former path Reuss Glacier
Lucerne
Lake Lucerne
Molasse
Meikirch
Napf 1408
Pilatus 2119
Bern
Möschberg
Aare
Helvetic Nappes
Thalgut
Molasse
Hohgant 2197
Brienzer Rothorn 2350
Titlis 3238
Thun
Subalpine Molasse
Brienz
Meiringen
Penninic Nappes
Lake Brienz
former path Aare Gl.
Innertkirchen
Lake Thun
Stockhorn 2190
Spiez
Interlaken
Schwarzhorn 2928
Guttannen
Niesen
(Para-) Autochthonous Mesozoic
Handegg
Jungfrau 4158
Finsteraarhorn 4274
Crystalline
Blüemlisalp 3657
A
Germany
France
Austria
Switzerland
Slovenia
Italy
LGM extent
Elevation [m a.s.l.]
4680
-50
C
moraine
drumlin
Depth below surface
1 m
217 m
Kander before 1714
Thun
Aare
Fig. 3
Fig. 4
Fig. 2
Beatenberg
Beatenbucht
Sundlauenen
Spiez
Interlaken
Lombach
Aare
Lütschine
Kander
Simme
Niesen
0 1.5 3 km

130

Fig. 1A) Ice extent covering the Alps during the Last Glacial Maximum (LGM). Extent of the ice sheet is taken from Ehlers and Gibbard (2004). Elevation data created from SRTM 1 Arc-Second (courtesy of the U.S. Geological Survey). B) Hill-shade of digital elevation model (swissALTI3D from swisstopo) with ice altitude during LGM superimposed (Bini et al., 2009). White contour lines mark relief elevation. Lake Thun was covered by 650 m (Thun) to 850 m (Interlaken) of ice with respect to current lake level. Former glacial path is indicated (white line), arrowheads show Gschnitz and Egesen stadial positions during deglaciation (Wirsig et al., 2016). The main tectonic units are labelled. Red rectangle in A) shows extent of map. C) Hill-shade of digital elevation model with swath bathymetry of Lake Thun and some of the most prominent glacial landforms (GeoCover dataset, swisstopo).

1.2. Previous seismic surveys

A first seismic study on Lake Thun was performed by Matter et al. (1971), following the technical recommendations of Hinz et al. (1970) who had previously used the same equipment to investigate Lake Zurich in 1968. The successful imaging and interpretation of the bedrock surface in Lake Thun resulted in a structural map of the basin. They noticed that the deepest part of the lake coincides with a local, spatially well confined depression in bedrock topography to more than 500 m below lake level, adjacent to a shallow-water platform towards Interlaken, where bedrock was interpreted at ~100 m depth below water surface. Drill hole lithology at Interlaken Hospital, however, revealed at that depth the transition between lake sediments and older gravels and sands (Bodmer et al., 1973). In contrast, Bodmer et al. (1973) interpreted bedrock at 300 m below surface in their onshore seismic refraction campaign on the western edge of the Interlaken plateau. Independent of the bedrock depth underestimation, Matter et al. (1971) recognized in their seismic data a few distinct seismic stratigraphic horizons: a shallow one between 7–10 m below the lake bottom, which was attributed to the impact of the Kander deviation from 1714 CE, and two additional ones at 90 and 130 m in the northwestern part of the lake and 100 and 190 m in the deep lake basin. They suggest that the oldest deposits in the Lake basin have pre-LGM ages, as it was subsequently shown for the deposits at Thalgut between Thun and Bern (Schlüchter, 1989b).

Finckh et al. (1984) surveyed 17 perialpine lakes using air-gun seismic reflection profiles in combination with sonobuoy refraction measurements in order to evaluate the importance of glacial erosion for perialpine lake formation and the preservation potential of pre-LGM deposits. They single out a few distinctive horizons and assign an overall stratigraphic pattern across all perialpine lakes, which consists of an upper and lower glacio-lacustrine infill and bedrock. In some cases, as for Lake Thun, they split the lower glacio-lacustrine infill into three subunits. The thickness and seismic velocities ranging from 1450 m/s (water column) to 2330 m/s (lowermost sedimentary infill) are in good agreement with this study (see Table 1). They conclude that the erosion of bedrock can be assigned to older glacial periods, since the glacial advance during LGM overrode older glacio-lacustrine deposits revealing only slight loading and erosion, so that deposits of previous glacial cycles are preserved.

The upper 60 m of the sedimentary infill of Lake Thun have been described in detail by Wirth et al. (2011) using high-resolution single-channel pinger data. The artificial deviation of the Kander River in 1714 CE created a sudden increase in sediment supply to Lake Thun, the formation of a new delta, the accumulation of sediment on existing delta slopes and hence a frequency increase in mass-movement-related turbidites which are represented by large units of a chaotic/transparent seismic facies.

*Table 1: Overview of seismic campaigns on Lake Thun. * Assuming sufficient signal power in the filtered frequency range and a velocity of 1500 m/s (Rayleigh's criterion of λ/4; e.g. Widess, 1973).*

Acquisition year	1969	1984?	2007	2015
Source type & vol. [cm^3] *refraction*	Air gun 100–200	Air gun 83 *83–655*	3.5 kHz pinger	2-chamber air gun 2 x 245.8
Shot interval [s]	1	5–7	0.5	10
Survey type	Reflection	Reflection & *Refraction*	Reflection	Reflection
# of channels, streamer length (spacing)	1, -	?, 15	1, -	24, 92 (4 m)
BP freq. filtering [Hz]	-	50–600 *20–50*	2200–6300	52-80-1500-2200
Vel. analysis, interval Vel. for infill [m/s]	None, 1500	*Refraction, 1450–2330*	None, 1450	NMO-analysis, 1430–2100
Vert. resolution [m]	?	0.6–7.5*	0.1–0.2	0.7–2.5
Shot spacing [m] at speed [m/s]	1.4–2.5 at 1.4–2.5	?	0.55 at 1.1	(2m CMP distance)
Total profile length	102 km	?	70 km	183.5 km
Publication	Matter et al. (1971)	Finckh et al. (1984)	Wirth et al. (2011)	this publication

2. Methods

2.1. Reflection seismic survey

Acquisition

We conducted a multi-channel reflection seismic survey on Lake Thun and used a Sercel two-chamber Mini GI airgun (15/15 in^3) in combination with a Geometrics MicroEel streamer of 97 m length and 24 channels (4 m channel distance with 3 hydrophones per channel) as acquisition tools and recorded 42 lines with over 180 km total length. Recording of seismic data was nonstop and turns were included into the interpretation software up to 90° deviation from the main course of each line. In order to supplement quality control and data interpretation, brute-stacks were analyzed with a bin width of 12 m, bin distance of 4 m, low and high cut-off frequencies of 20–30 Hz and 1000–1500 Hz respectively, NMO of 1500 m/s and time migration.

Table 1 gives an overview of all seismic campaigns carried out on Lake Thun. The setup used in this survey overcomes the drawbacks of limited resolution and penetration depth, using state-of-the-art equipment and processing work flow. Shot time interval was 10 seconds at 6.6 km/h survey speed, resulting in an average shot spacing of 18 m and an assigned common-mid point (CMP) interval of 2 m, corresponding to half the receiver spacing. The frequency spectra show reasonable signal power up to 500 Hz, resulting in a vertical resolution of the topmost stratigraphic sequences of $\lambda/4 = 0.7$ m. An average theoretical vertical resolution of $\lambda/4 = 2.5$ m is obtained, when using a velocity of 1500 m/s and a main frequency of 150 Hz (Widess, 1973; Chopra et al., 2006) . The GI gun yielded significanty higher resolution when compared to previous airgun surveys (e.g. Finckh et al., 1984). The position of the survey vessel was tracked with a Garmin GPSmap76Cx GPS receiver recording one point every 2 s with 2–5 m accuracy. Since the survey velocity was kept constant during acquisition, the easting and northing positions were individually smoothed and interpolated to 1 s. The smoothing was done with a local regression using weighted linear least square and a first degree polynomial model. Shot timing was recorded with an onboard GPS clock. After CMP assignment, the tracks were Kalman-filtered before integration into the interpretation software *SMT Kingdom Suite 2015*.

Processing

The following processing steps were applied to the seismic data with the processing software *SeisSpace/ProMAX (Halliburton/Landmark)*: frequency bandpass filtering, muting, velocity-model creation based on normal-move-out (NMO) analysis and recorded sound-velocity profiles from bathymetric survey, multiple suppression using surface-related multiple elimination (SRME; Verschuur et al., 1992), NMO corrections and CMP stacking, post-stack FX-deconvolution, and post-stack Kirchhoff depth migration.

The velocity estimate for the water column was based on the average of 39 P-wave profiles recorded during the bathymetric campaign in September 2014, the direct wave from seismic data and information from a water station at Thun. Only the topmost 40 m of the water column change significantly throughout the year. The velocity in 1 m water depth was calculated from the direct wave travelling along the floating streamer. The estimated velocity is about 1435 m/s based on 5 shots of each survey line. In 5 m water depth, the formula of Wong and Zhu (1995) was applied, which uses temperature [°C], salinity [ppt] and pressure [kPa] as input to calculate sound speed. Salinity was assumed to be zero. Additionally, we consulted the water temperature recordings of the Aare discharge station located close to Lake Thun (3 km downstream from the outlet), which are continuously provided by the Federal Office for the Environment (FOEN). The calculated velocity in 5 m water depth is 1434.2 m/s. The profile between 0 and 70 m was then interpolated in a cubic manner.

NMO velocity analysis ideally requires strong continuous horizontal reflections, which is not always given. Velocities for up to 7 reflections (lake bottom to top bedrock) at every 100th to 200th CMP were picked, depending on the length of the profiles and the morphology of the bedrock. Bedrock velocity was kept below 2500 m/s, since the migration algorithm can handle only moderate lateral velocity changes. In overdeepened lake basins where water-saturated low-velocity sediments are in direct contact to bedrock, downward and lateral velocity increases from 1500 m/s to 4000 m/s and higher are common and beyond the capabilities of the migration algorithm. However, our underestimated bedrock velocities affect primarily bedrock-internal structures which are mostly beyond the resolution and focus of our study.

Major challenges were encountered close to the shoreline, where water depth is only a few tens of meters and surface-related multiples were difficult to remove, as the SRME algorithm revealed its limitations. Due to the rather short streamer length, the CMP-fold was often as low as 2 or 3, but the low fold had a negligible impact on the image quality due to the high quality of the data.

2.2. Multibeam bathymetry

High-resolution bathymetry data of Lake Thun were acquired during 14 days in September and October 2014 (Fig. 1C) using a Kongsberg EM2040 multibeam echo sounder. The positioning system used for the bathymetric campaign was a Leica GX1230 GNSS receiver in combination with the swipos GIS/ GEO real-time kinematic positioning service provided by swisstopo. Survey lines were oriented mostly parallel to the lake's long axis, while areas of shallow water depth (< 15 m) were surveyed in a shore-parallel pattern. Bathymetric data cover most of the lake basin from the deepest areas up to 5 m water depth. The processed point cloud has been rasterized for geomorphologic analysis of the lake floor. The resulting digital bathymetric map has a cell size of 1 m with a vertical accuracy in the order of a few decimeters. Hilbe et al. (2011) and Hilbe and Anselmetti (2014) provide a more detailed review on the acquisition procedure, equipment setup and the use of swath bathymetry tools in lake research.

3. Seismic stratigraphy

3.1. Introduction

The overall seismic stratigraphy of Lake Thun shows, from bottom to top, a succession of bedrock, glacial tills, glacio-lacustrine and lacustrine deposits. This general stratigraphy can be further subdivided into ten seismic units (U0–U9), based on characteristic seismic facies, unconformities and predominantly prominent strong reflections (Figs. 2, 3 and 4). However, seismic facies may change within one single unit, but units are not subdivided further for simplicity reasons. All stratigraphic sequences are clearly discernable in the deep basin (Fig. 2), where reflections are laterally continuous and bedrock morphology reveals major overdeepening with steep flanks. Recognition of single sequences is impeded when approaching the gas-rich delta deposits of the river Kander and its signal blanking characteristics (Fig. 3). About 400 m beyond the rim of the eastern platform towards Interlaken, signal penetration fades out and the shallow water depth causes strong multiples making it impossible to trace units into the center of the platform. Close to river inlets, gas-rich sediments prohibit good signal penetration as well.

Table 2 provides an overview of the seismic stratigraphic interpretation. Since lithological and sedimentological information is lacking, the stratigraphic interpretation is mainly based on hydroacoustic data and derived from morphological, geometric properties of the facies.

261 *Table 2: Seismic stratigraphy in Lake Thun with facies, max. unit thicknesses, geometry description, expected lithology and interpretation.*

Unit	Seismic facies (max. thickness in shallow basin NE/deepest basin SW)	Expected lithology	Interpretation
U9	Similar as U8 (> 100 m on subaquatic platform in the E)	Lacustrine deposits with few turbidites and coarse gravely base with clays intercalated	Similar as U8 with increased fluviatile influence
U8	Parallel, strong continuous horizontal reflections, with semi-transparent intercalated sections (40 m/60 m)	Lacustrine sedimentation (sand to clay) with intercalated turbidites	Increasing *in-situ* sediment production, Holocene
U7	Transparent facies with only gentle horizontal reflections, onlapping (20 m/20 m)	Normally graded layer, possibly pebbles at base	Mass-movement-induced megaturbidite
U6	Parallel, strong continuous reflections with onlap onto U5 or deeper units, amplitudes laterally varying towards NW, faults (~50 m/~50 m)	Mostly sandy silt and mud, strong layering, turbidites	Lacustrine deposits, high sedimentation rate due to proximity of melting glacier
U5 (1A-8A)	High-amplitude reflections with faint internal stratification, layering slightly inclined outside main basin dipping to E	Diamict, sand, gravel, boulders	Build-up of terminal moraine crest of stagnant, or slightly readvancing glacier
U5 (1B-7B)	High-amplitude, continuous reflections in foresets to bottom sets at top of sequence; base of each subunit with rather chaotic facies, few faults rooting in deeper units (20 m/100m)	Mostly sand and glacial mud, with coarse material at the base	Transition from proximal (till) to more distal fine-grained glacio-lacustrine deposition, overall coarsening towards proximal positions
U4	Horizontal reflections with generally low amplitudes, laterally varying, onlapping onto U3, few faults (-/80 m)	Fine laminated muds with dropstones, melt-out from glacier base, deposition from suspensions	Glacio-lacustrine sediments, no ice contact, initiation of deglaciation
U3	Transparent to semi-transparent chaotic facies at the base with faint internal stratification, higher amplitudes towards the top with disturbed layering, many faults, overall similar to U1 (~50 m/~150 m)	Diamict with dropstones at base, fining up with glacial mud towards the top	Waterlain till with shore-parallel eskers on the flanks
U2	Semi-transparent facies at bottom, high-amplitude reflections at the top (especially N of Spiez), strong continuous inclined layering, deformed and eroded by U3, many faults (20 m/50 m)	Bottom: proximal diamict with coarser fraction; Top: fine muds	Partially stratified (deformed) till, eroded by subsequent glacial readvance, temporal subglacial lake development
U1	Transparent to semi-transparent chaotic facies, generally low amplitudes, few faults (-/>160 m)	Diamict, glacial mud with dropstones, coarse gravelly base	Oldest glacial sediments, till, esker-like features on the SW flank of the basin
U0	High-amplitude, laterally continues reflections in NW, low-amplitudes in SE and greater depth, strongly inclined internal reflections	Molasse, limestone, globigerina marls, dolomite, gypsum, clays	Bedrock of subalpine molasses, Penninic and Helvetic nappes

262

3.2. Unit U0 – bedrock

U0 is interpreted to represent the bedrock below the lake. The top of the unit displays numerous morphologic steps and is marked by a series of high-amplitude reflections in the north, fading out towards the south and at greater depth.

The bedrock often comprises inclined reflections typical for Penninic and Helvetic nappes (Wissing and Pfiffner, 2002). Syn- and antiforms occur in the vicinity of the transition from Penninic nappes to Subalpine Molasse in the northwestern part of the basin (Fig. 3). The bedrock surface reveals a complex morphology with the most pronounced incision south of Beatenberg at roughly 750 m below today's lake surface. The incision narrows at Beatenbucht (Fig. 1C), where limestone formations crop out in vertical cliffs, as well as close to the sill at Spiez, where an antiform on land extends into Lake Thun (Fig. 3). Distinct valley troughs, causing a local secondary inset trough within the basin (Fiore et al., 2011), were cut into the bedrock and probably represent erosional imprints of highly erosive subglacial meltwater flows (Menzies and Shilts, 2002; Fig. 4). Fig. 6 shows the surface of the bedrock U0 with depth and morphological information. The deepest point reaches 776 m below lake level (557.48 m a.s.l.) with an elevation of 218 m below sea level. Based on the recorded 42 seismic lines (Fig. 7A), the sedimentary infill was calculated to amount to >560 m in the deepest part of the basin (Fig. 7B).

3.3. Unit U1 – till 1

Unit U1 reveals a broad range of facies and is capped by a rather discontinuous reflection (Fig. 2, etc.). The facies ranges from transparent to semi-transparent with occasional faint internal stratification. U1 overlies bedrock (U0) and is spatially restricted to the deepest part of Lake Thun. It pinches out towards the sill at Spiez (Fig. 7C), filling up a distinct bedrock trough. As in Lake Zurich (Giovanoli et al., 1984), this pattern is interpreted as till lacking coherent reflectors and resulting in a nearly transparent facies.

U1 levels out some of the bedrock channels and shows itself a diverse morphology with local peaks at the flanks. Highly reflective, arc-shaped peaks up to ~15 m in height are stacked on the southeastern flank of line 08 (Fig. 3). These positive subglacial landforms could represent subglacial channel fills, (e.g. eskers), infilled with stratified gravelly deposits (Pugin et al., 1999; Fiore et al., 2011). There are almost no faults recognizable due to limited signal penetration and decreasing resolution with depth.

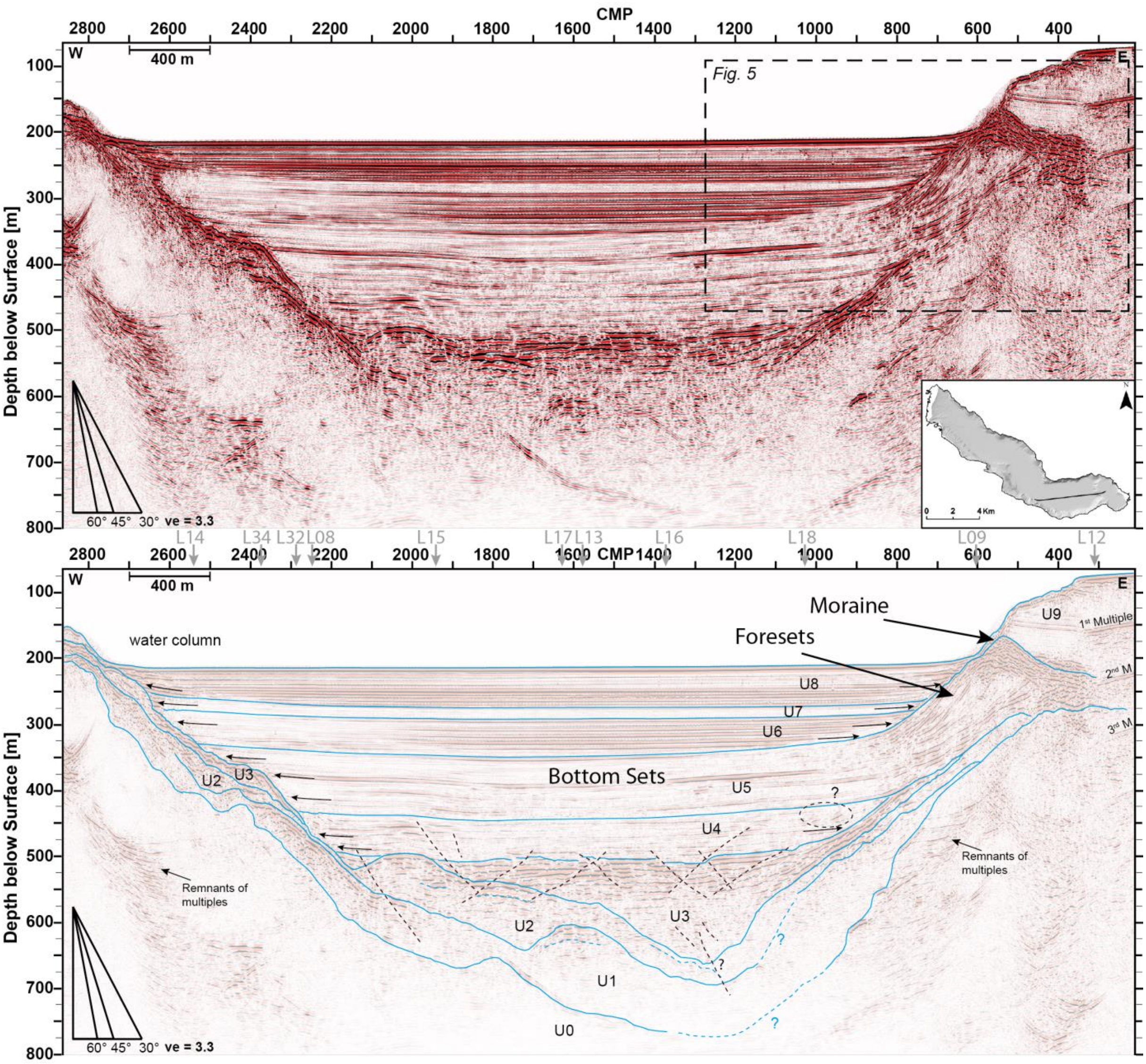

Fig. 2: Seismic inline profile 20 along the deepest section of the basin shows all stratigraphic units interpreted to represent bedrock (U0), sub- to proglacial deposits (U1-U5), and glacio-lacustrine to lacustrine (U6-U9) deposits. The profile track is shown in the inset (top). Beyond the platform in the East, signal loses penetration due to the shallow waters and strong multiples. Remnants of multiples are visible in some other parts of the profile. The moraine and its related foresets and bottom sets in U5 are illustrated in more detail in Fig. 5. Small black arrows mark onlapping. The black question mark highlights inclining layers within horizontal deposits. Many faults populate U2 to U5 (black dotted lines). Grey arrows show intersections with crosslines.

3.4. Unit U2 – (stratified) till 2

Unit U2 is characterized by a general increase of high-amplitude continuous reflections compared to subglacial till unit U1, which is increasingly well-developed towards the top of the unit and in the NW (Fig. 3). While these seismic facies is likely to reflect an internal bedding of unit U2, some similarity with the chaotic facies U1 is apparent.

The origin of stratification in tills may be sedimentary or deformational. In overdeepened glacial basins, stratified deposits typically represent either waterlain tills emplaced in a dynamic subglacial to sub-marginal lake setting (see also U3) with temporary loss of glacier ground contact, or alternatively, an incompletely stratified unit U2 due to subglacially deformed and overridden glacio-lacustrine deposits, which preserved some of the initial stratification. 133 individual fault strands penetrate U2 with the majority located in the NW (Fig 3). However, the size of the faults (several tens of meters) is beyond the commonly expected extent for subglacial deformation (range of decimeters, Boulton et al., 2001). The non-uniform thickness of the unit and local troughs suggest that U2 was partially deformed and eroded by a subsequent glaciation (Fig. 2). We suggest both, the combination of a deformational and a sedimentary origin of the stratification, which is indicated by the subhorizontal internal bedding and the infilling character that levels out underlying topographic undulations of U1 and U0. The unit covers the entire basin except the shallow platform close to Interlaken. Since U1 is not present NW of the sill at Spiez, U2 directly overlies the bedrock there. Some patches of U1 occasionally occur SE of the sill at Spiez (Fig. 3). Unit U2 can be therefore interpreted as stratified till in a subglacial environment.

3.5. Unit U3 – (waterlain) till 3

Unit U3 shows a transparent to semi-transparent facies at the base with only slight internal stratification. Towards the top of the unit, higher amplitudes start to dominate and the facies change into a similar character as U2. The layering is frequently disturbed by faults. In the deepest part of the basin, the reflections are mostly horizontal, while the deposits on the flanks show a slope-parallel inclination. The base of U3 reaches elevations down to 100 m below sea level in the South. U3 mostly levels out the undulating topography of underlying units. Similar to U1, the highly reflective, arc-shaped peaks occur at the very same flank in profile 08 (Fig. 3) and are up to ~25 m high. They are traceable across several lines with a shore-parallel extension and possibly represent a chain of eskers (Pugin et al., 1999; Fiore et al., 2011).Unit U3 is more extensive than U1 and covers almost the entire basin (Fig. 7D).

The base of U3 is interpreted as the onset of the last glaciation with an erosive base removing partially underlying U2, causing a non-uniform thickness distribution and undulating top of U2, and emplacing a glacial till (Lister et al., 1984). The relatively smooth and continuous top of U3, with a pronounced horizontal character at the deepest section of the basin, therefore indicates terminal deposits that have not been overprinted by a subsequent glacial readvance with deforming ice contact at the base. However, the high amplitudes underlining the horizontal internal layering of U3 in line 20 (Fig. 2) tends to be slightly exaggerated, since some of this horizontality has to be attributed to the partial lack of multiple removal. Nevertheless, the deepest part of the basin is dominated by high-amplitude horizontal reflections, signaling the potential loss of ground contact of the glacier and the onset of the development of a subglacial to sub-marginal lake (Fig. 2). Line 08 and 31 in Figs. 3 and 4 illustrate the undulating internal stratification of U3.

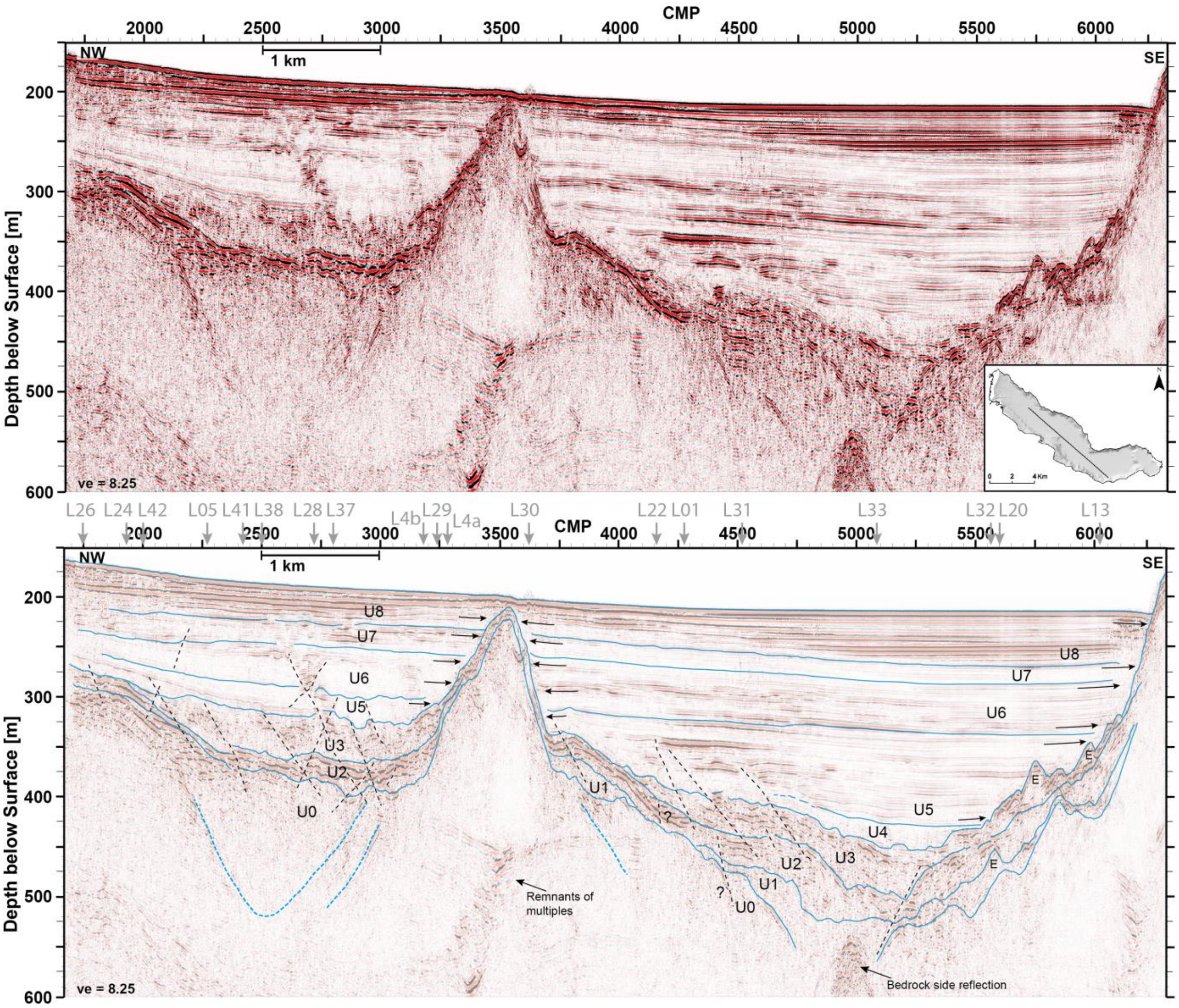

Fig. 3: Seismic inline profile 08 across the sill at Spiez. The profile track is shown in the inset (top). Towards the NW, signal loses penetration due to gas rich sediments brought by the Kander river. U1 and U4 are missing NW of the sill. Blue dotted lines hint at syn-/antiforms in the bedrock. Black arrows mark onlapping. "E"s show esker-like structures.

Most of the faults observed in our data (167 individual fault strands out of 193 totally identified strands) penetrate U3. About one third of all fault strands are thrust faults with apparent dip angles lower than 35°, and one quarter shows a normal faulting regime. The remaining strands do not allow for a specific faulting regime to be identified or have to be interpreted as strike-slip faults. Brittle faulting is commonly observed in subglacial tills and typically associated with low basal shear stresses and low pore-water pressures. However, the observed faults may be of neotectonic nature rooting in bedrock structures, since the subglacial deformation zone is usually limited to a few decimeters (e.g. Boulton et al., 2001; Piotrowski et al., 2001) and therefore beyond the seismic resolution. Alternatively, the faults may be related to the sediment overload (settlement) induced by the infill or a postglacial rebound as described at a larger scale for the Fennoscandian ice sheet (Muir-Wood, 1989, 2000).

3.6. Unit U4 – post-LGM subglacial lake sedimentation

Unit U4 shows mostly horizontal low-amplitude reflections onlapping onto U3, indicating an abrupt change in the depositional environment. The unit is clearly restricted to the southeastern part of the basin (Figs. 3 and 4) and has a seismic facies comparable to U5.

During deposition of U3, the glacier loses eventually contact with the ground or simply disintegrates and retreats. U4 records the time between a lifted and retreating Aare glacier (U3) and ice-free conditions with the ice front at the subaquatic platform (see U5) or further upstream. Initially, U4 is mostly deposited from rain-out of a melting ice tongue, suspension settling and sediment flows producing finely laminated muds with dropstones (Bennett and Glasser, 2009). In Fig. 2, faint traces of inclined layers are recognizable (marked with a dashed circle), likely related to the onset of clinoform formation (see U5) as it is typical for the sediment dumping in front of a nearby glacial tongue. This depositional regime translates soon thereafter to a glacio-lacustrine to lacustrine environment in a proglacial lake.

3.7. Unit U5 – Sundlauenen subaquatic moraine complex (SMC) and clinoforms

In case of unit U5, the excellent data quality allowed for a further subdivision into subunits 1 to 8, each of them made of a corresponding package characterized by distinct seismic facies, marked with a letter suffix A and B (Fig. 5). The two types of seismic facies and its division into eight subunits are best seen on line 20 (Figs. 2 and 5). Facies A builds arc-shaped crests with high-amplitude reflections with partial internal stratification. It extends from the north to the south shore along the platform edge (inset Fig. 5 bottom). Facies B is characterized by high-amplitude continuous reflections steeply inclined close to the crest and becoming gradually less inclined and eventually horizontally layered in the center of the basin. U5 was deposited over the entire basin (Fig. 7E).

Based on the arc-shaped and dome-like geometry, as well as reflection characteristics, facies A is interpreted as subaquatic moraine complex, hereafter termed Sundlauenen subaquatic moraine complex (SMC), created by a stagnant to periodically readvancing glacier during its overall retreating phase. Its vertical thickness at the peak of the moraine crest amounts to ~130 m. Very similar facies and structures in correspondence with recessional glacial phases are known from lake and fjord settings (e.g. Lønne and Syvitski, 1997; Waldmann et al., 2010; Hilbe et al., 2011).Thrust faults within facies A are likely to form during minor readvances/oscillations when the glacier pushes into the morainal ridges as commonly observed in terminal moraine settings (e.g. Lønne and Syvitski, 1997; Bennett, 2001; Johnson et al., 2013). Similar subaquatic moraine features, documenting readadvance periods during LGM deglaciation, were reported for Lake Neuchâtel (Ndiaye et al., 2014) and Lake Geneva (Fiore et al., 2011).

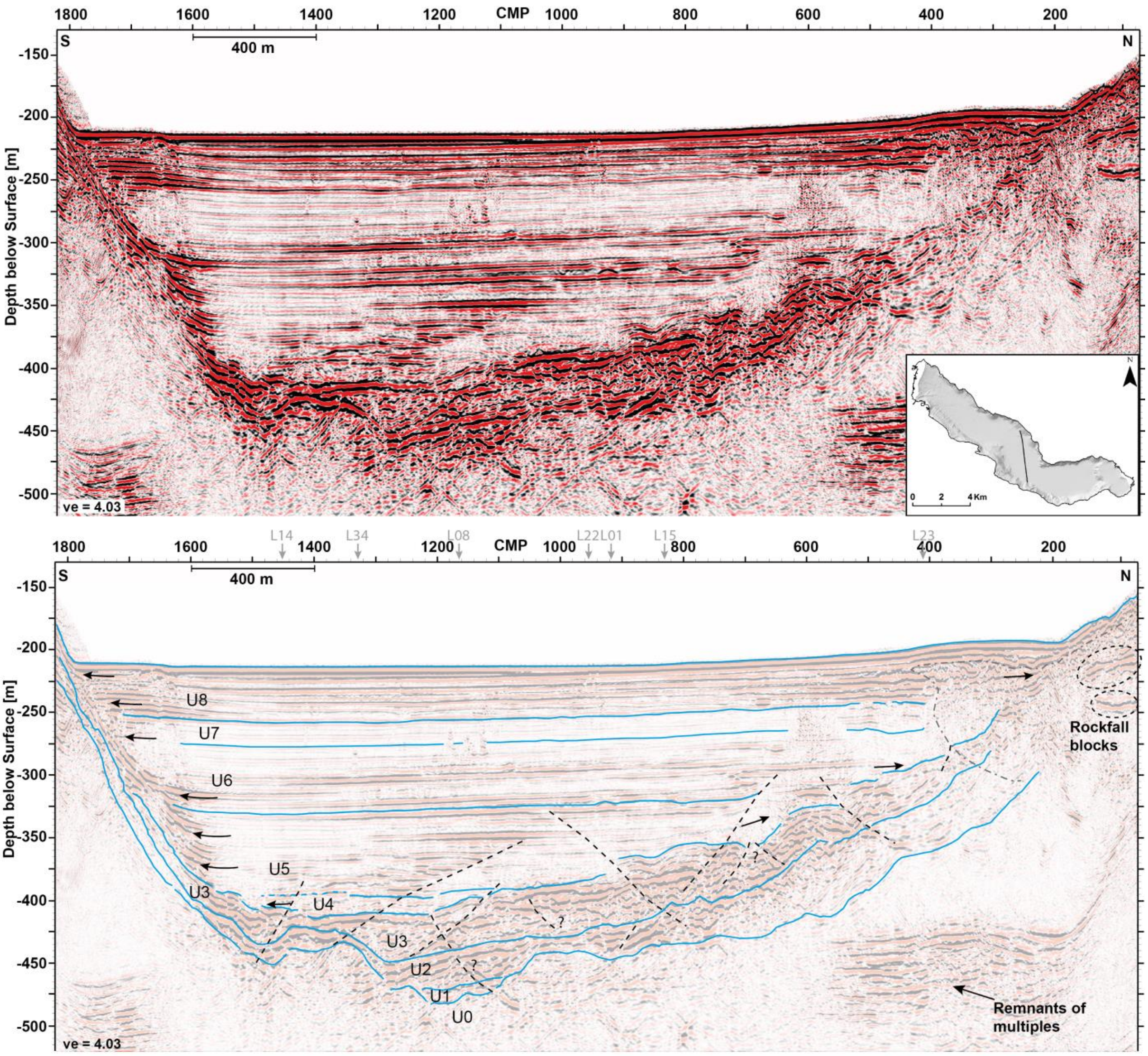

Fig. 4: Seismic crossline profile 31. The profile track is shown in the inset (top). Towards the N, signal loses penetration due to the Ralligen rockfall 588/599 CE (see also Wirth et al., 2011). Blocks of limestone belonging to the rockfall are marked with black dashed circles. The dashed dotted grey line outlines the rockfall affected area. Black arrows mark onlapping and black dashed lines indicate faults.

Facies B is interpreted to be glacio-deltaic clinoforms that originate close to the moraine crest and represent foresets at the ice-distal slope and bottom set beds in the deepest part of the basin.

Subunits A and B are deposited simultaneously (Fig. 5) forming a genetic seismic sequence. Adapting a seismic sequence stratigraphic approach, these subunits can be defined as 'subaquatic glacial seismic sequences', which allow the reconstruction of glacial retreat and advance stages and ice front positions during an ice-grounded moraine formation. Dip angles of the foresets, as well as tratigraphic thicknesses increase during the initial phase of the SMC build-up (subunits 1–4) and start to decrease thereafter (subunits 5–7).

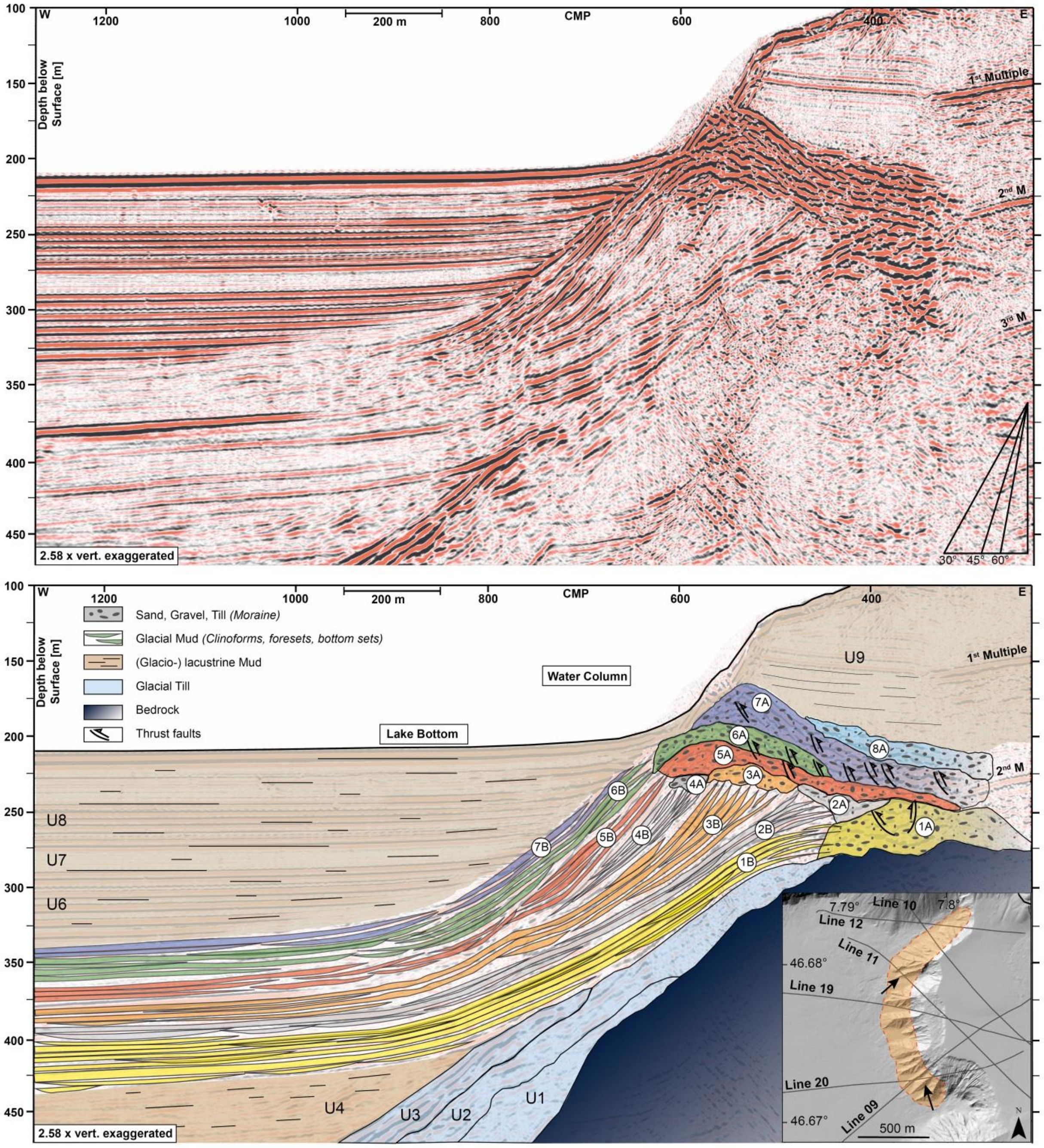

Fig. 5: Numerals 1–8 mark individual subdivisions of unit 5 in line 20 (Fig. 2). Corresponding letters A,B indicate different facies of subunits. Top: Blue dotted lines mark package boundaries of subunits. Inset: Overview of subaquatic moraine extension (orange area) delineated by seismic and swath bathymetry data. Upper and lower bounds of orange area are drawn along moraine apexes of 7A (seismic) and toe of lake-bottom slope. The orange polygon measures ~200 m across and 1.6 km along the arc. Black arrows mark remnants of high-amplitude erosion-resistant moraine crests.

The combined thickness of U4 and U5 (Fig. 7E) marks the sedimentation during the onset of deglaciation in the deepest part of the basin. It amounts to ~170 m of sediment, which represents a third of the entire sedimentary column.

3.8. Unit U6 – glacio-lacustrine deposits

In the deepest part of the basin, unit U6 is dominated by high-amplitude parallel reflections (Fig. 2), which lose amplitudes towards the flanks. The transparency of the reflections also increases constantly towards the NW (Fig. 3) and the reflections finally fade out entirely when approaching the Kander delta.

The facies of U6 is characteristic for sedimentation in a low-energy, glacio-lacustrine environment. During its formation, the lake is entirely ice-free, and the largest sediment fraction delivered to the lake is provided by glacio-fluvial melt water of the retreating Aare Glacier, and to some minor parts, by smaller tributaries. Initially, the ice front might have been still in contact with the lake water in the form of a floating glacier tongue. However, the basin of Lake Brienz, separated by progradation of a tributary delta (Lombach & Lütschine river) upstream of the subaquatic moraine crest soon becomes an efficient sediment trap and hinders glacio-lacustrine material being transported beyond Interlaken, so that in-situ lacustrine sediment production becomes dominant.

3.9. Unit U7 – megaturbidite

Unit U7 shows a highly transparent seismic facies with only very slight layering. The sharp upper and lower boundaries of the unit (Fig. 2) occur in the deepest part of the basin all the way to the bedrock sill at Spiez. Beyond the sill further northwest, the transparency of the facies is replaced by higher amplitudes (Fig. 3). However, also in the northwestern part, the transparent facies persists, though it is limited to the base of U7. Generally, the unit is deposited across the entire basin apart from the subaquatic platform and the shallow bedrock sill at Spiez (Fig. 7F). The top of U7 reveals a smooth topography.

The highly transparent facies of U7 is typical for turbidites in general, but also for ‘megaturbidites’ and has been reported in several peralpine lakes such as Lake Como, Italy (Fanetti et al., 2008), Lake Geneva (Kremer et al., 2012) or Lake Lucerne (Schnellmann et al., 2006). The exceptional thickness and large extent clearly classifies it as a ‘megaturbidite’ (Bouma, 1987). The spatial extent of the ‘megaturbidite’ with significant thickness change beyond the bedrock sill at Spiez suggests that the sill itself acted as an efficient barrier. The turbidite had to flow around the bedrock barrier significantly slowing it down and leading to the reduced thickness and extent in the northwest (Fig. 3).

The source area of the turbidite is located close to the bedrock escarpment (Fig. 7F, I) where a spatially restricted chaotic facies dominates and penetrates and affects U6 locally. However, the expected massive limestone blocks related to the big escarpment and the ancient rockfall (rockfall at Balmholz, ~0.1 km3, Beck, 1907) are no longer recognizable on seismic data and must have been removed by a former glaciation. Therefore, a subsequent smaller subaerial or subaquatic rockfall most likely caused the 'megaturbidite'. Rockfall-evolved mass-flow deposits and associated 'megaturbidites' have been previously reported in other perialpine lakes as in Lake Lucerne (Schnellmann et al., 2006).

3.10. Unit U8 & U9 – lacustrine deposits

Unit U8 is characterized by high-amplitude reflections with small semi-transparent to transparent intercalations. The unit extends over the entire basin and is analyzed and described by Wirth et al. (2011).

Unit U9 is limited to the lacustrine deposits on the subaquatic platform close to Interlaken. The seismic facies is comparable with U8 and contains an alternation of high-amplitude reflections and intercalated semi-transparent deposits. Signal penetration in the center of the platform is hampered by the shallow water depth and its associated multiples. This effect is additionally enhanced by gas-rich sediments. Therefore, internal facies and structures of U9 are solely resolved close to the platform edge (Fig. 2).

Unit U8 was affected by several mass movements and contains their related turbidites. Mass movements were induced by lake-level fluctuations, floods, nearby earthquakes and delta-slope instabilities (Wirth et al., 2011). Blocks of the Ralligen rockfall in 598/599 CE (Wirth et al., 2011) are visible in the bathymetric data in form of raised limestone blocks surrounded by a semi-circular lobe of squeezed out and deformed lake sediments (Fig. 1C). The blocky and chaotic character of the seismic profiles crossing the mass-movement deposit confirms these observations (Fig. 4). The source area of the associated mass-flow deposit is given in Fig. 7F, II.

Similarly, U9 is also influenced by subaquatic mass-movement deposits recognizable in the bathymetric data (Fig. 1C). However, the U8 and U9 stratigraphy are not directly comparable with each other since the moraine complex in U5 acts as a trap and sediment barrier for incoming fluvial material form the east brought by the Aare, Lütschine and Lombach rivers. Especially the latter two delivered a lot of coarse gravely material (Bodmer et al., 1973) and silted up the area at Interlaken, creating a fundament of fluvial deposits in U9 and shifting later towards a lacustrine dominated deposition.

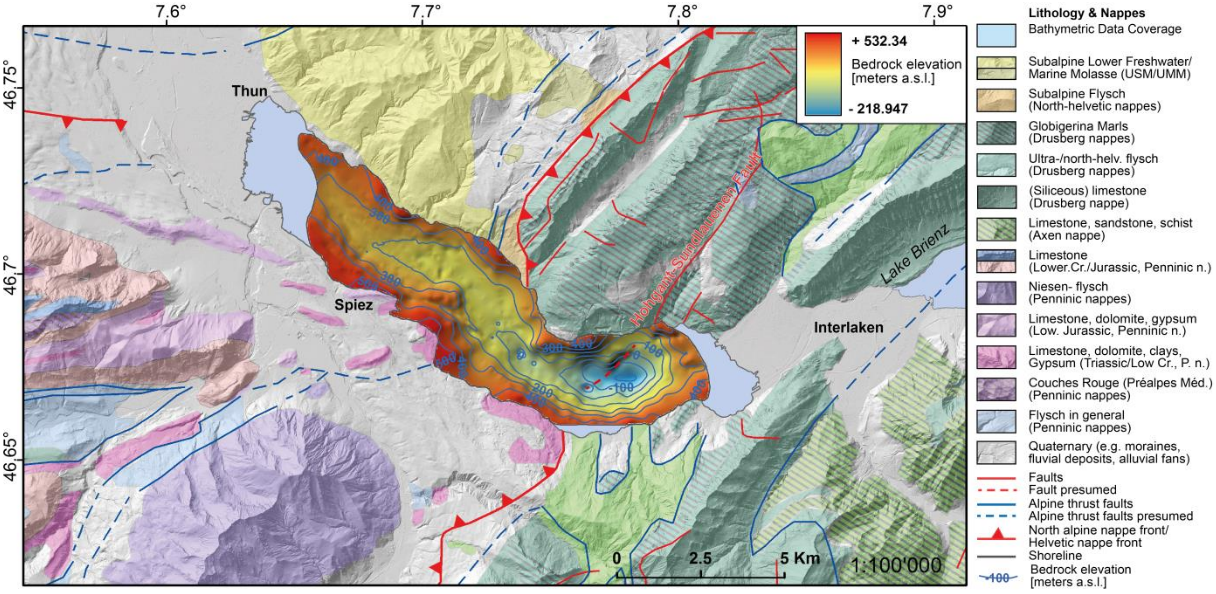

Fig. 6: Hill-shade of digital elevation model (swissALTI3D from swisstopo) with color-coded bedrock map (25 m cell size FlexGridding algorithm, Kingdom Suite 2015) and local geology (simplified Geologie 500 map from swisstopo) superimposed. 100 m contour interval is added for readability. Bright blue zone reflects the data coverage by the bathymetric campaign.

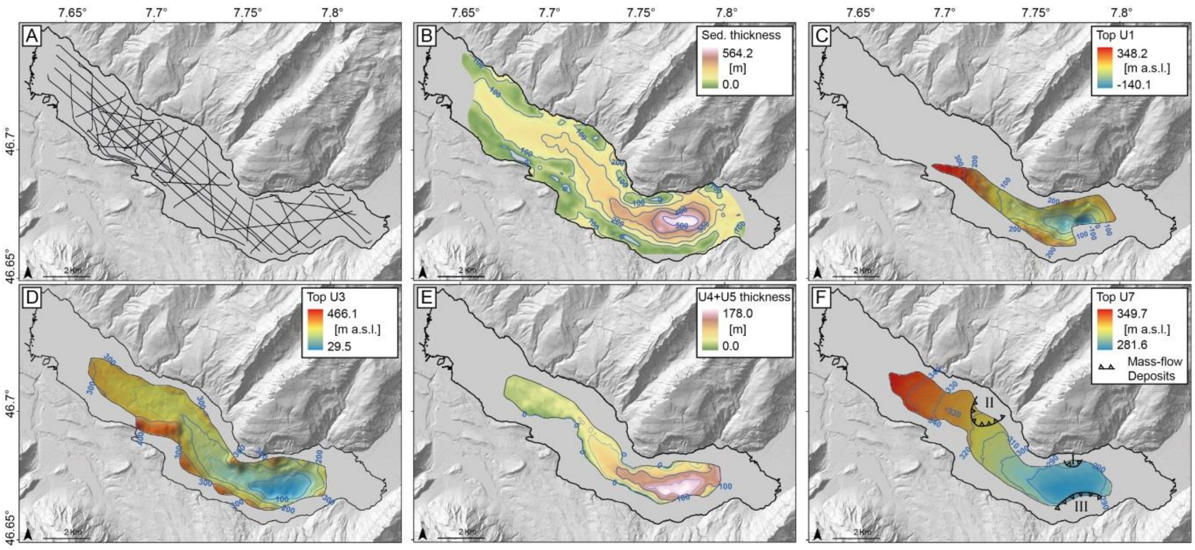

Fig. 7: A) Multi-channel reflection seismic line tracks. B) Calculated sediment thickness based on the difference of swath bathymetry data and the bedrock map; C) Extent and morphology of the top U1, the lowermost till deposits. D) Extent and morphology of the youngest till deposit. E) Thickness of U5, the deltaic clinoforms and its directly underlying sediment U4. U4 is mostly restricted to the deepest basin. F) Extent of top U7. Source area of mass-flow deposit I, II and III are in U7, U8 and U8, respectively. All gridded horizons are limited to the extent of the seismic lines where the corresponding picked horizon was encountered in order to reduce extrapolation of data to a minimum

and only interpolate between the lines. We converted all horizons to a 25 m grid (FlexGridding algorithm, Kingdom Suite 2015) for the calculations. Thick blue contours show intervals of 100 m, except for F) with 10 m intervals.

4. Discussion

4.1. Bedrock morphology

The overall shape of the bedrock surface in the lake basin is in good agreement with the results from (Matter et al., 1971). However, we obtained a significantly larger overdeepening (776 vs. ~550 m) in the deepest section with respect to the current lake/base level at 557.48 m a.s.l. Matter et al. (1971) likely interpreted the strongest reflection as bedrock, which we identified as top of unit U3. The seismic survey of Lake Brienz led to similar values in its deepest section with an overdeepening exceeding 800 m (Matter et al., 1973), even though they used a constant velocity of 1500 m/s, which is assumed to significantly underestimate bedrock depth. Finckh et al. (1984) reported an overdeepening of 605 m for Lake Thun, which is ~150 m less than what we observed for the deepest depression. This deviation is mainly due to the course and orientation of the profile in Finckh et al. (1984), which is slightly offset to the east with respect to the deepest point in bedrock. The massive bedrock depression observed in Lake Thun is in good agreement with many other overdeepened basins in the Alps (e.g. Preusser et al., 2010).

The overdeepening of more than 750 m at the deepest point (i.e. −200 m a.s.l, Fig. 6) in the Lake Thun basin (with lake level as reference) can be attributed to multiple supporting factors. First, we propose that there is a possible lithological bedrock control. The northern shoreline is dominated by Globigerina Marls (Helvetic nappes) and in the south by Flysch (Helvetic n.), dolomite, gypsum and clays (Triassic and Penninic n.). These bedrock types are rather sensitive to erosion and can be easily removed by the erosional power of subglacial meltwater.

Secondly, there is a tectonic control via Hohgant-Sundlauenen fault (Fig. 6) that caused a synsedimentary extensional movement (Breitschmid, 1978) with a displacement of up to 1025 m in Cretaceous-Eocene times (Häuselmann, 2002) and provides a weak zone supporting the creation of the overdeepened basin. A prolongation of the fault into Lake Thun is very likely and depicted in Fig. 6. The bedrock elevation drop in the lake at the presumed continuation of the fault amounts to 240 m. These observations suggest that the overdeepening was caused by a combination of subglacial erosional processes and tectonic predisposition (Preusser et al., 2010; Dürst Stucki and Schlunegger, 2013). Towards the NW, bedrock rises to higher elevations: at the drilling site Thalgut, 10 km NNW of Thun outside the lake, bedrock was encountered at 147 m below surface. Figs. 3 and 6 illustrate this continuously rising bedrock surface from the deepest point of the basin towards the outlet. Reber and Schlunegger (2016) calculated the thickness of Quaternary sediments of 100–150 m underneath the city of Thun. According to their model, bedrock then stays at fairly constant elevation with a slight descent towards Bern. From the deepest basin towards Interlaken, bedrock rises steeply at ~26° and peaks at 200 m below surface, building a barrier that hosts the platform and the subaquatic moraine.

4.2. Timing of glacial deposition (till 1 to 3)

The time of emplacement of the thick glacial deposits (U1–U3) can only be done in a qualitative way, since there is no deep drill core data available from Lake Thun for temporal classification. U3 is the youngest glacial unit and covers the entire basin, therefore we attribute it to LGM. The older sequences U1 and U2 cannot be put into temporal context with the data at hand. Generally, two plausible scenarios can be imagined:

1) A multi-cycle concept, where U1 and U2 belong to independent pre-LGM glacial cycles, as it is documented for the Aare valley at nearby drill site Thalgut (Schlüchter, 1989a; 1989b; see Fig. 10 for location) or known from the drill site at Lake Zurich (Lister et al., 1984) with four till sequences that are all topped by glacio-lacustrine sediments deposited in a lacustrine (subglacial) environment. Also Lake Annecy and Lake Le Bourget, France, host remnants of pre-LGM sediments (Van Rensbergen et al., 1998; van Rensbergen et al., 1999). U1 and U2 most likely postdate the mid-Pleistocene, since Häuselmann et al. (2008) unraveled evidence for five glacial advances in the Aare valley within the last ~220ka based on dated speleothems.

2) A multi-phase single cycle concept, where U1 and U2 are part of the last glaciation. Fiord-type lakes in British Columbia, Canada, and the New York Finger Lakes show that sediments predating the last glacial cycle must have been entirely eroded and only massive diamicts of several hundred meters thickness witness the last glacial cycle (Eyles et al., 1991; Mullins et al., 1996; Eyles and Mullins, 1997).

While U3 signals a grounded glacier, which eventually starts to lift off the ground, retreat and disintegrate, U4 was deposited temporally between the abandonment of the LGM position and the halt of the glacier to form a "quasi-stagnant", slightly fluctuating ice front at Interlaken. Since U4 is restricted to the deepest basin, a subglacial lake developed most likely within this short time frame, with subglacial meltwater and glacier melt-out providing most of the glacio-lacustrine sedimentary input. The rapid disintegration and readvance left no time for a basin-wide deposition of lacustrine sediments.

4.3. Depositional concept of the Sundlauenen subaquatic moraine complex (SMC)

The interpretation of Fig. 5 can be approached in two different ways:

SMC Model 1

The conceptual model created by Lønne (1995) for ice-contact submarine fan systems and the corresponding ice-front advance-retreat (mini-)cycles — we introduce here the term mini-cycle to avoid confusion with major glacial cycles — applies also to glacio-lacustrine environments. These systems often show a slow advance phase, a short stillstand of the glacial front, followed by a rapid disintegration (Meier and Post, 1987; Lønne and Nemec, 2011). One complete mini-cycle holds five allostratigraphic units, defined on the basis of outcrops, seismic sections and ground-penetrating radar, which they then applied to temperate glaciers in Norway (Lønne, 1995; Lønne and Syvitski, 1997; Lønne, 2001; Lønne and Nemec, 2011). We slightly adopted their scheme to three allostratigraphic units to fit best with our observations. The subscript “L” stands for “Lønne” to avoid confusion with nomenclature used in this study. They list the units of a mini-cycle in a seismic or outcrop section as follows from bottom to top:

A_L ice-contact facies during glacier advance (foresets coarsening upfan, bottomsets intercalated by sandy turbidites, including syn-sedimentary glacio-tectonic deformation, erosion)

B_L ice-contact facies during glacier stillstand/retreat (foreset beds, bottom set beds, boundary A_L/B_L erosive in the upper part and concordant towards the bottom sets, deformation/erosion on ice-proximal slope possible)

C_L ice-distal facies formed during retreat (sediment from meltwater deposited over entire ridge, no deformation)

A_L-B_L-C_L resembling one glacial mini-cycle are partly relatable to the Sundlauenen subaquatic moraine in Fig. 5. To be most in accordance with the scheme introduced by Lønne (1995) and Lønne and Syvitski (1997), subunits 1 A/B to subunits 4 A/B would all belong to a phase A_L, ice-contact facies formed during glacial (re)advance. This is mainly based on the forestepping character of the subunits A with respect to each other. After 1A/B to 4A/B, it follows a period of glacial stillstands and or slight retreats with subunits 5A/B to 7A/B mainly based on the thick accumulation of 5A, 6A and 7A on the ice-proximal slope and the relative location of the crests to previously deposited material indicating backstepping. Allostratigraphic unit C_L is not recognizable, either because most of it has been reworked and used in the subsequent readvance, or the thickness of the subunit is beyond the resolution of the seismic data. This second part of the mini-cycle is terminated by 8A, what is called $\mathrm{B}t_L$ and interpreted as basal ice-contact facies, showing the last retreating stage and the final abandonment with the *termination* of the mini-cycle. This is followed by the deposition of unit C_L, ice-distal sediments signaling the final retreating stage, represented by the base of units U6 and U9 (in summary the mini-cycle would be A_L-A_L-A_L-A_L-B_L-B_L-B_L-$B\mathit{t}_L$-C_L).

SMC Model 2

A different approach would be to tie each single depositional package made of subunits A & B as a readvance that might be followed by a short phase of stillstand (Fig. 8A). Readvance/stillstand were not necessarily always interrupted by a retreating phase, since a stillstand can be directly followed by a renewed advance. However, the clear separation of individual packages, including the fact that foresets and bottom sets of single packages show a low-amplitude base and reveal clearer high-amplitude reflections towards the top (Fig. 5), suggests that the sediment emplacement was not continuous throughout time. It was relatively more significant at the onset of deposition and ceasing with time until an interruption occurred during short phases of smaller or larger retreats accompanied by sediment dumping to the proglacial area (Fig. 8B). The sediment dumping occurs likely in the form of turbiditic events in the proximal slope area. The bottom set beds most likely contain intercalated mass-movement related turbidites and fluvial input from tributaries, as the sudden glacial retreat promotes slope instabilities. Any moraine material deposited at the top of the ridge or in the proglacial area during a readvance of the glacier is eventually overrun and partially eroded, remobilized and reused to form a new crest during a subsequent readvance (Fig. 8C). Hence, what we observed are rather pulses of readvances, occasionally interrupted by short retreats with no deposition (Lønne and Nemec, 2011), resembled by every single package rather than a continuous succession of deposits through time. Therefore, every single package could reflect a short (re)advance-retreat mini-cycle, totaling to seven such cycles. Eventually, climatic conditions change and final abandonment of the stadial position takes place with ice-distal sedimentation primarily at the ice-proximal slope side of the crest (Fig. 8D,E).

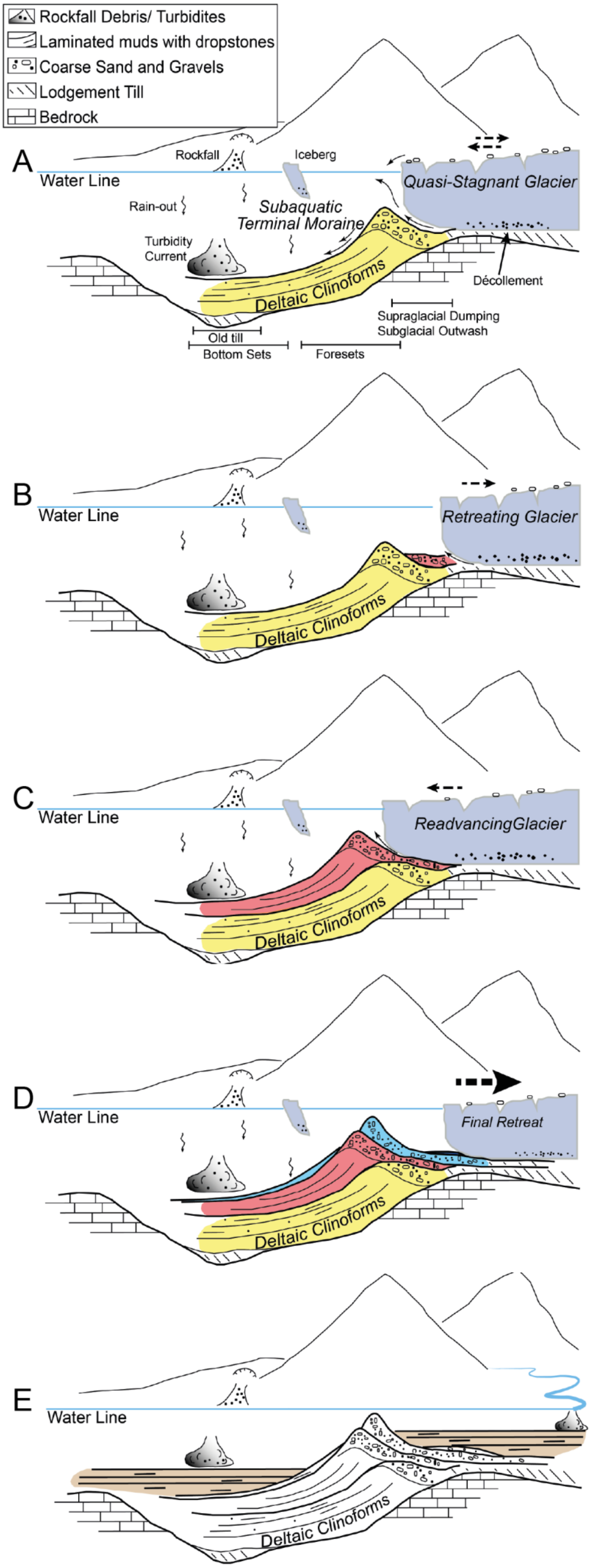

Fig. 8: Conceptual model illustrating the relative chronology of the recessional phase of the Aare Glacier. A) Stagnant or slightly readvancing phase. B) Retreating phase. C) Readvancing phase and moraine and deltaic clinoform build-up. Previous moraine crest is overridden and partially eroded. D) Rapid retreat. E) Complete abandonment of stadial position. Glacio-lacustrine, but mainly lacustrine and fluvial sedimentation dominate.

614

It is important to note that the stratigraphic thickness of the bottom sets is to some extent correlated to the thickness of the till placed at the top of the crest. E.g. 1A) in Fig. 5 shows a thick deposit of till and hence also a thick sequence of bottom sets. 4A) is almost non-existent and hence there is hardly any bottom sets distinguishable that can be assigned to 4B).

Combination of SMC Models 1 & 2

Fig. 9 summarizes the two presented conceptual models above based on measurements taken from seismic sections 09 and 20. Fig. 9 (left panel) shows the reconstructed ice-front movements, based on the positions of individual moraine crests in U5 of line 20. The location of the subaquatic grounded glacial front is picked at the location of the peak of each crest. The cumulative bottom set thickness was measured in the deepest basin of line 20. Subunits 1–4 show a prograding system with each new moraine crest being placed further downstream, formed by an advancing glacier that overruns previous deposits. Single subunits are well distinguishable in seismic data, suggesting a stagnant period of the glacier towards the end of an advancing phase, which is possibly followed by a short retreat (Fig. 9 grey dotted lines) before the initiation of a readvance. Subunits 5–7 show an aggrading/retrograding system with crest formation mainly during a stagnant phase or shortly after a small retreat followed by a readvance.

The dip angles of the foresets are measured on line 09, since the orientation of the line is perpendicular to the strike direction of the SMC (Fig. 5 inset). Line 20 displays apparent dips which differ from the true values measured on line 09. The right panel in Fig. 9 shows that dip angles steepen during the build-up of the complex (subunits 1–4) and start to decline thereafter (subunits 5–7). Similarly, the bottom set thickness increases during build-up and starts to cease in the aggrading/retrograding phase. Subunit 4 shows the steepest foresets, but no bottom set deposits are recognizable due to the limited resolution in the seismic data set or a phase of almost no deposition in the deep basin, indicating a dramatic change in accommodation space (forestepping to backstepping) leading to sediment starvation in the basin.

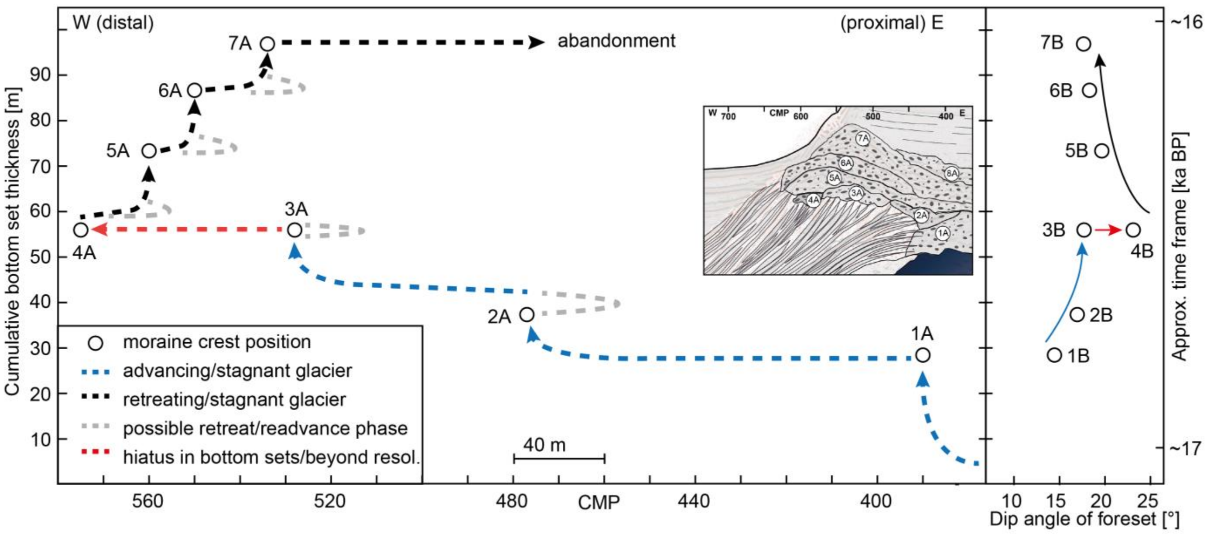

Fig. 9: Left panel: Ice-front movements based on moraine crest positions in U5 of line 20 (see extract from Fig. 5), plotted versus cumulative bottom set thickness taken at CMP 1600 in line 20. Right panel: Right panel: Dip angles taken close to the moraine crests at the steep onset of the forests in line 09. Median of 10 measurements is plotted with a standard error smaller than the circle size. Steepening of the angles during overall glacial advance and flattening during overall retreat.

Hence, the thickness of the bottom sets is related to the sediment productivity of the system, which is a function of time, sediment availability and efficiency in sediment mobilization (sub-, supra-, en- and proglacially). The controls on accommodation space and the depositional pattern are not so much driven by changes in relative lake level or tectonic movements, as it is the case in a typical marine setting (e.g. Catuneanu et al., 2011), but are rather tied to the behavior of the ice front (single pulses of advance, stillstand, retreat), which cause forestepping, upstepping and backstepping. The bottom set beds of U5 represent almost 1/5 of the entire infill thickness (~ 550 m), indicating high sedimentation rates, followed by a rapid disintegration, which may be even comparable to the down-wasting observed since the end of the 20th century (Paul et al., 2007).

The material for the build-up of the SMC is provided by two sources: subglacial diamict material from the deforming layer the glacier sits on and/or basal till and outwash material from meltwater outflow (Lønne, 1995). Apart from the re-mobilization of subglacial material and proglacial sediments along a basal gliding plane (décollement), the complex might be additionally promoted by ice-marginal glacial dumping, glacial thrusting (thrust faults in Fig. 5 bottom) and meltout (Bennett and Glasser, 2009). Whatever process dominated the build-up, the formation of the SMC was involved a number of different processes.

4.4. Deglaciation

The deglaciation history of the Aare valley since the Last Glacial Maximum is constrained by a limited set of absolute ages illustrated in Fig. 10. Akcar et al. (2011) dated an erratic boulder to 19 ±

0.9 ka at Möschberg (T1 in Fig. 10) applying cosmogenic nuclide surface-exposure dating (erosion-corrected ^{10}Be age). At least until this time, the Aare valley was covered by a thick valley glacier. Wirsig et al. (2016) obtained a robust minimum exposure age of 17.7 ± 0.8 ka for the onset of the deglaciation. The timing of ice-free conditions is given by the radiocarbon-dated calcareous clay gyttja from 8.3 m depth in Late-Glacial Lake Amsoldingen, located adjacent to the water outlet of Lake Thun. It shows an age of ~16.3 ka BP (Lotter, 1985), providing a minimum age for an ice-free area at the small lake (T2 in Fig. 10).

Furthermore, the Late-Glacial retreat of the Aare Glacier into its high-Alpine catchment upstream of Lake Thun was investigated by Wirsig et al. (2016). They modelled the Aare Glacier ice extent combining glacial striae, trimline elevations with surface exposure ages and GIS ice surface models. Their most conservative model for the Gschnitz stadial resulted in a terminal position of the Aare Glacier as far downstream as Interlaken between Lake Brienz and Lake Thun. However, models with less shear stress on the bed agrees better with their observed striae and elevation patterns suggesting a terminal position at Innertkirchen between 17–16 ka (T4 in Fig. 10), which might represent the Gschnitz stadial (Wirsig et al., 2016, recalculated from Ivy-Ochs et al., 2006). On the basis of ^{10}Be exposure ages of boulders from the end moraine at the type locality at Trins (Austria), Ivy-Ochs et al. (2006) dated the Gschnitz stadial to 15.4 ka ± 1.4 ka. Glacial readvance was initiated about 500 years earlier and is expected to emplace significant moraine crests, which to date are missing, hidden or not preserved for many larger glaciers such as the Aare Glacier. In the Aare valley, the end position for the next younger stadial, the Egesen stadial at 12.9–11.5 ka (T5 in Fig. 10, Wirsig et al., 2016) lies between Handegg and Guttannen.

Neither model by Wirsig et al. (2016), with T4 at Interlaken or at Innertkirchen can explain the obtained scatter in exposure ages (13.6–16.1 ka) from boulders and bedrock samples at a local through shoulder at a high-altitude site (Gelmerhörner ridge). Currently, Wirsig et al. (2016) assume a local remaining ice patch has covered the ridge during Gschnitz stadial or toppling and spalling leads to the scatter. Alternatively, this might be tackled with a model suggesting a terminal moraine position beyond Interlaken (e.g. at T3), causing an elevated ice coverage to an altitude that is in better agreement with the observed ^{10}Be ages at Gelmerhörnli.

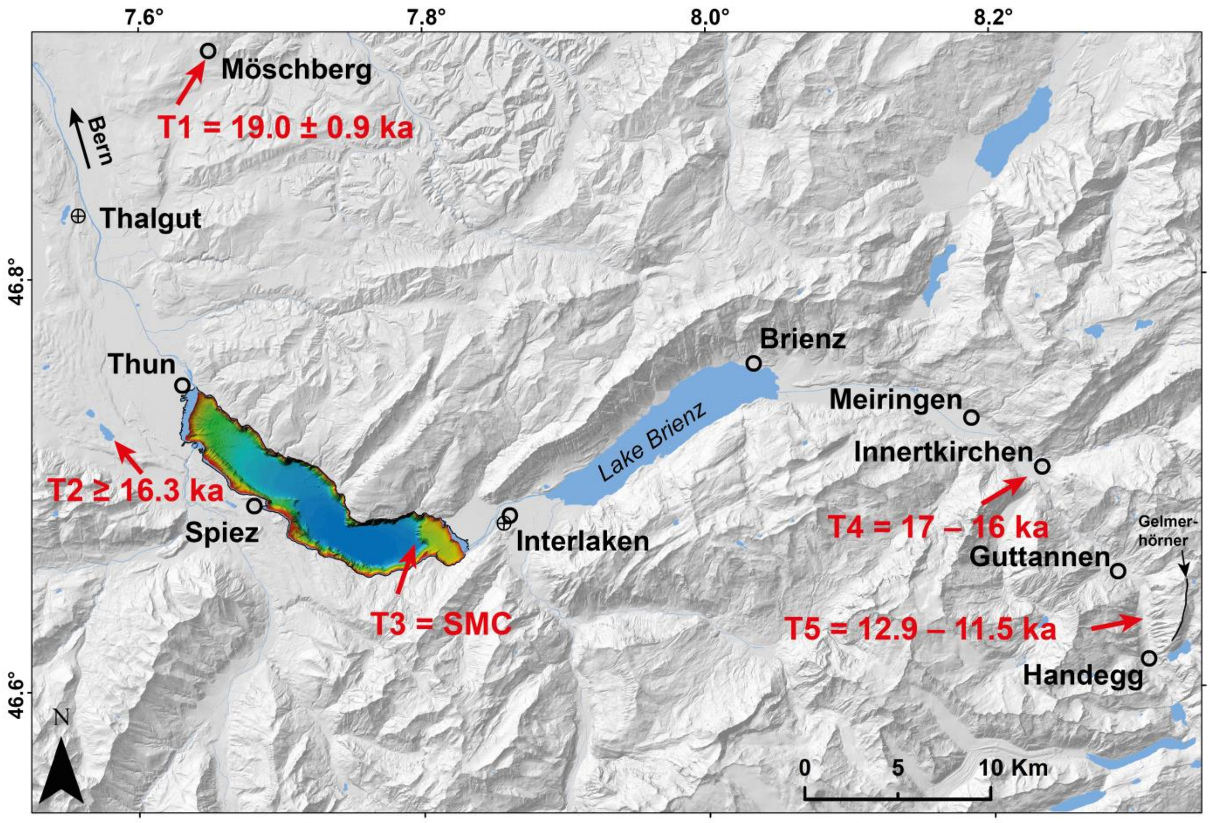

Fig. 10: Overview of available age constraints regarding the deglaciation stages of the Aare Glacier between LGM and the Younger Dryas. The crossed circles indicate drilling sites Thalgut and Interlaken Hospital. See text for more details.

The time window for the Aare Glacier to retreat from T1 to T5 amounts thus to ~5,200 – 8,400 ka. The calibrated radiocarbon age (using IntCal13, Reimer et al., 2013) of T2 of ~16.3 ± 0.3 ka cal BP age (uncalibrated ^{14}C-age 13.49 ka ± 0.17, calibrated 2-sigma range is 16,801–15,769 years BP, Lotter et al., 1985) gives rather a lower bound and is most likely underestimating the age. But assuming the onset of the deglaciation of the Aare valley occurred no later than 17.7 ka, the available time window for the glacier tongue to recede ~80 km from Bern (17.7 ± 0.8 ka) all the way upstream to Innertkirchen (T4, 16.5 ± 1.4, dating error from Ivy-Ochs et al., 2006) amounts to 1.2 ± 1.6 ka. Hence the time window for the formation of the SMC narrows to less than 1,000 years. This suggests that the Aare Glacier disintegrated rapidly, similar to the fast ice-collapse of the Garda glacial amphitheater as proposed by Ravazzi et al. (2014), and was accompanied by extraordinary high sedimentation rates. The combined thickness of U4 and U5 (Fig. 7E) amounts to ~175 ± 10 m in the deepest basin, accumulated between the abandonment of the Aare Glacier's LGM position (19.0 ± 0.9 ka) and the position at Innertkirchen (16.5 ± 1.4 ka). This conservative estimation leads to a sedimentation rate of 7.0 ± 0.7 cm/yr. If we consider U5 separately, apply the assumption above and take into the calculation ~100 ± 5 m of bottom set sediments deposited in less than 1.2 ± 1.6 ka, we obtain a sedimentation rate of >8.3 ± 1.3 cm/yr during SMC formation. This seems a reasonable estimate for a rapidly disintegrating Aare Glacier, as the sedimentation rate in Lake Zurich immediately after glacial withdrawal ~17 ka ago was calculated to be ~11 cm/yr (Lister et al., 1984). However, better time constraints could possibly result in a sedimentation rate even twice as high.

5. Summary and conclusions

Using the combination of multibeam bathymetry data and multi-channel reflection seismic data, we present a new bedrock map of the Lake Thun basin, highlighting the importance of an accurate velocity model in order to obtain correct depth values. The overdeepened bedrock incision reaching 770 m below today's lake surface or down to ~220 m below current sea level is in agreement with other perialpine lakes. Bedrock incision is the result of a combination of forces primarily represented by subglacial meltwater and glacial scouring. It was additionally promoted by stratigraphic and tectonic predisposition providing erosion-prone bedrock formations and pre-existing deformation features, such as the Hohgant-Sundlauenen fault.

The multi-channel reflection seismic data allowed a detailed seismic stratigraphic analysis. Ten units (U0–U9) have been identified. The uppermost waterlain till (U3) belongs to the last glaciation. Underlying till units (U1, U2) are either part of the last glaciation and signal changes in the depositional environment (multi-phase single cycle) or, more likely, represent independent remains of pre-LGM glacial cycles. The subsequent unit U5 illustrates an intermediate halt during a dramatic recessional phase of the Aare Glacier. The detailed seismic stratigraphic analysis revealed a to-date unknown subaquatic moraine complex and its internal architecture in the Lake Thun basin. Its eight subunits are distinct individual depositional packages indicating local fluctuation of the ice front with single pulses of advance and retreat distinguishable.

The two presented conceptual models for the build-up of the Sundlauenen subaquatic moraine complex (SMC) represent two end-member scenarios. A combination of the two models that allows for individual (re)advance-retreat mini-cycles, despite the systematic lack of deposits signaling clear retreats due to re-mobilization of material, seems to fit best with our findings from the stratigraphic analysis. Existing age constraints indicate that the retreat of the Aare Glacier to its inner-Alpine region and the formation of the SMC occurred in less than 1,000 years, accompanied by sedimentation rates exceeding 8 cm/yr.

Further investigations are needed to constrain the timing of the deposition of the Sundlauenen subaquatic moraine complex within the Late-Glacial stratigraphy. Namely, whether the SMC can be correlated with stadial climatic deteriorations, e.g. the Gschnitz stadial that has been so far lacking in the major longitudinal valleys within the Alps, or it has to be considered as an exceptional occurrence that signals a so far unknown perturbation in an almost traceless deglaciation history.

Competing interest

The authors declare that they have no conflict of interest.

Acknowledgements

The processing of the seismic reflection data was performed with SeisSpace/ProMAX provided through Halliburton/Landmark's University Grant Program and the stratigraphy was interpreted with Kingdom Suite 2015.0 provided by IHS and. This work was partially financed by the building insurance of the Canton of Bern GVB and the Federal Office of Topography swisstopo. We are thankful for the collaboration with various people at Vigier Beton Einigen, with special thanks to Arnold Gertsch and Peter J. Haller and his team. We appreciated the technical support by Sven Winter during the seismic campaign. SRTM 1 Arc-Second data was provided by the U.S. Geological survey. We acknowledge the constructive comments of two reviewers.

References

Akcar, N., Ivy-Ochs, S., Kubik, P. W., and Schluchter, C., (2011) Post-depositional impacts on 'Findlinge' (erratic boulders) and their implications for surface-exposure dating. *Swiss Journal of Geosciences*, 104(3), p. 445-453.

Anselmetti, F. S., Drescher-Schneider, R., Furrer, H., Graf, H. R., Lowick, S. E., Preusser, F., and Riedi, M. A., (2010) A similar to 180,000 years sedimentation history of a perialpine overdeepened glacial trough (Wehntal, N-Switzerland). *Swiss Journal of Geosciences*, 103(3), p. 345-361.

Beck, P., (1907) Der diluviale Bergsturz von St. Beatenberg. *Mitteilungen der Naturforschenden Gesellschaft in Bern*.

Beck, P., (1920-1922) Grundzüge der Talbildung im Berner Oberland. *Eclogae Geologicae Helvetiae*, 16(2), p. 39.

Beck, P., (1933) Über das schweizerische und europäische Pliozän und Pleistozän. *Eclogae Geologicae Helvetiae*, 26(2), p. 335-437.

Bennett, M. R., (2001) The morphology, structural evolution and significance of push moraines. *Earth-Science Reviews*, 53(3), p. 197-236.

Bennett, M. R., and Glasser, N. F., 2009, Glacial Geology: Ice Sheet and Landforms, Wiley-Blackwell.

Bini, A., Buoncristiani, J.-F., Couterrand, S., Ellwanger, D., Felber, M., Florineth, D., Graf, H. R., Keller, O., Kelly, M., Schlüchter, C., and Schoeneich, P., (2009) Switzerland during the Last Glacial Maximum 1: 500'000. *Bundesamt für Landestopografie swisstopo.*

Bini, A., Cita, M. B., and Gaetani, M., (1978) Southern Alpine lakes — Hypothesis of an erosional origin related to the Messinian entrenchment. *Marine Geology*, 27(3), p. 271-288.

Bodmer, R., Matter, A., and Scheller, E., (1973) Geologische, seismische und pollenanalytische Untersuchung im Bödeli bei Interlaken. *Mitteilungen der Naturforschenden Gesellschaft in Bern*, 30), p. 14.

Boulton, G. S., Dobbie, K. E., and Zatsepin, S., (2001) Sediment deformation beneath glaciers and its coupling to the subglacial hydraulic system. *Quaternary International*, 86), p. 3-28.

Bouma, A. H., (1987) Megaturbidite - an Acceptable Term. *Geo-Marine Letters*, 7(2), p. 63-67.

Breitschmid, A., (1978) Sedimentologische Untersuchungen in der eocaenen Hohgant-Serie im Helvetikum nördlich von Interlaken. *Eclogae Geologicae Helvetiae*, 71), p. 143-157.

Buechi, M. W., Frank, S. M., Graf, H. R., Menzies, J., and Anselmetti, F. S., (2017) Subglacial emplacement of tills and meltwater deposits at the base of overdeepened bedrock troughs. *Sedimentology*, 64(3), p. 658-685.

Catuneanu, O., Galloway, W. E., Kendall, C. G. S., Miall, A. D., Posamentier, H. W., Strasser, A., and Tucker, M. E., (2011) Sequence Stratigraphy: Methodology and Nomenclature. *Newsletters on Stratigraphy*, 44(3), p. 173-245.

Chopra, S., Castagna, J., and Portniaguine, O., (2006) Seismic resolution and thin-bed reflectivity inversion. *CSEG recorder*, 31(1), p. 19-25.

Clark, P. U., Dyke, A. S., Shakun, J. D., Carlson, A. E., Clark, J., Wohlfarth, B., Mitrovica, J. X., Hostetler, S. W., and McCabe, A. M., (2009) The Last Glacial Maximum. *Science*, 325(5941), p. 710-714.

Dehnert, A., Lowick, S. E., Preusser, F., Anselmetti, F. S., Drescher-Schneider, R., Graf, H. R., Heller, F., Horstmeyer, H., Kemna, H. A., Nowaczyk, N. R., Zuger, A., and Furrer, H., (2012) Evolution of an overdeepened trough in the northern Alpine Foreland at Niederweningen, Switzerland. *Quaternary Science Reviews*, 34), p. 127-145.

Dürst Stucki, M., and Schlunegger, F., (2013) Identification of erosional mechanisms during past glaciations based on a bedrock surface model of the central European Alps. *Earth and Planetary Science Letters*, 384), p. 57-70.

Ehlers, J., and Gibbard, P. L., 2004, Quaternary glaciations-extent and chronology: part I: Europe, Elsevier.

Escher, H. C., (1820) Über die fremdartigen Geschiebe und Felsblöcke, welche sich in verschiedenen Ländern vorfinden, mit Hinsicht auf Herrn J.A. De Luc's des Jüngern in Genf hierüber aufgestellten Hypothese. *Annalen der Physik*, 65(5), p. 15

Eyles, N., and Mullins, H. T., (1997) Seismic-stratigraphy of Shuswap Lake, British Columbia, Canada. *Sedimentary Geology*, 109(3), p. 283-303.

Eyles, N., Mullins, H. T., and Hine, A. C., (1991) The seismic stratigraphy of Okanagan Lake, British Columbia; a record of rapid deglaciation in a deep ‘fiord-lake’ basin. *Sedimentary Geology*, 73(1), p. 13-41.

Fanetti, D., Anselmetti, F. S., Chapron, E., Sturm, M., and Vezzoli, L., (2008) Megaturbidite deposits in the Holocene basin fill of Lake Como (Southern Alps, Italy). *Palaeogeography Palaeoclimatology Palaeoecology*, 259(2-3), p. 323-340.

Fiebig, M., Herbst, P., Drescher-Schneider, R., Luthgens, C., Lomax, J., and Doppler, G., (2014) Some remarks about a new Last Glacial record from the western Salzach foreland glacier basin (Southern Germany). *Quaternary International*, 328), p. 107-119.

Finckh, P., Kelts, K., and Lambert, A., (1984) Seismic Stratigraphy and Bedrock Forms in Perialpine Lakes. *Geological Society of America Bulletin*, 95(9), p. 1118-1128.

Finckh, P. G., (1978) Are southern Alpine lakes former Messinian canyons? — Geophysical evidence for preglacial erosion in the southern Alpine lakes. *Marine Geology*, 27(3), p. 289-302.

Fiore, J., Girardclos, S., Pugin, A., Gorin, G., and Wildi, W., (2011) Wurmian deglaciation of western Lake Geneva (Switzerland) based on seismic stratigraphy. *Quaternary Science Reviews*, 30(3-4), p. 377-393.

Fiore, J. T., 2007, Quaternary subglacial processes in Switzerland: Geomorphology of the Plateau and seismic stratigraphy of Western Lake Geneva: University of Geneva.

Giovanoli, F., Kelts, K., Finckh, P., and Hsü, J., (1984) Geological framework, site survey and seismic stratigraphy In: Quaternary geology of Lake Zurich: An interdisciplinary investigation by deep-lake drilling. *Contributions to Sedimentology*, 13), p. 5-20.

Haeuselmann, P., Granger, D. E., Jeannin, P. Y., and Lauritzen, S. E., (2007) Abrupt glacial valley incision at 0.8 Ma dated from cave deposits in Switzerland. *Geology*, 35(2), p. 143-146.

Häuselmann, P., 2002, Cave Genesis and its relationship to surface processes: Investigation in the Siebenhengste region (BE, Switzerland) [PhD Dissertation]: University Freiburg (Switzerland), 170 p.

Häuselmann, P., Lauritzen, S. E., Jeannin, P. Y., and Monbaron, M., (2008) Glacier advances during the last 400 ka as evidenced in St. Beatus Caves (BE, Switzerland). *Quaternary International*, 189), p. 173-189.

Heim, A., (1894) Ueber das absolute Alter der Eiszeit. *Vierteljahrsschrift der Naturforschenden Gesellschaft in Zürich*, 39), p. 180-186.

Hilbe, M., and Anselmetti, F. S., (2014) Signatures of slope failures and river-delta collapses in a perialpine lake (Lake Lucerne, Switzerland). *Sedimentology*, 61(7), p. 1883-1907.

Hilbe, M., Anselmetti, F. S., Eilertsen, R. S., Hansen, L., and Wildi, W., (2011) Subaqueous morphology of Lake Lucerne (Central Switzerland): implications for mass movements and glacial history. *Swiss Journal of Geosciences*, 104(3), p. 425-443.

Hinz, K., Richter, I., and Sieber, N. P., (1970) Reflexionsseismische Untersuchungen im Zürichsee. Teil 1: Geophysik. *Eclogae Geologicae Helvetiae*, 63(2), p. 511-523.

Hughes, P. D., Gibbard, P. L., and Ehlers, J., (2013) Timing of glaciation during the last glacial cycle: evaluating the concept of a global 'Last Glacial Maximum' (LGM). *Earth-Science Reviews*, 125), p. 171-198.

Ivy-Ochs, S., (2015) Glacier Variations in the European Alps at the End of the Last Glaciation. *Cuadernos De Investigacion Geografica*, 41(2), p. 295-315.

Ivy-Ochs, S., Kerschner, H., Kubik, P. W., and Schlüchter, C., (2006) Glacier response in the European Alps to Heinrich Event 1 cooling: the Gschnitz stadial. *Journal of Quaternary Science*, 21(2), p. 115-130.

Ivy-Ochs, S., and Kober, F., (2008) Surface exposure dating with cosmogenic nuclides. *Quaternary Science Journal*, 57(1-2), p. 179-209.

Ivy-Ochs, S., Schafer, J., Kubik, P. W., Synal, H. A., and Schluchter, C., (2004) Timing of deglaciation on the northern Alpine foreland (Switzerland). *Eclogae Geologicae Helvetiae*, 97(1), p. 47-55.

Jäckli, H., (1962) Die Vergletscherung der Schweiz im Würmmaximum. *Eclogae Geologicae Helvetiae*, 55(2), p. 285-294.

Johnson, M. D., Benediktsson, I. O., and Bjorklund, L., (2013) The Ledsjo end moraine-a subaquatic push moraine composed of glaciomarine clay in central Sweden. *Proceedings of the Geologists Association*, 124(5), p. 738-752.

Kelly, M. A., Ivy-Ochs, S., Kubik, P. W., von Blanckenburg, F., and Schluchter, C., (2006) Chronology of deglaciation based on Be-10 dates of glacial erosional features in the Grimsel Pass region, central Swiss Alps. *Boreas*, 35(4), p. 634-643.

Kerschner, H., Ivy-Ochs, S., and Schluchter, C., (1999) Paleoclimatic interpretation of the early Late-glacial glacier in the Gschnitz valley, central Alps, Austria. *Annals of Glaciology, Vol 28*, 28), p. 135-140.

Kremer, K., Simpson, G., and Girardclos, S., (2012) Giant Lake Geneva tsunami in AD 563. *Nature Geosci*, 5(11), p. 756-757.

Lister, G. S., Giovanoli, F., Eberli, G., Finckh, P., Finger, W., He, Q., Heim, C., Hsu, K. J., Kelts, K., Peng, C., Sidler, C., and Zhao, X., (1984) Late Quaternary Sediments in Lake Zurich, Switzerland. *Environmental Geology*, 5(4), p. 191-205.

Lønne, I., (1995) Sedimentary Facies and Depositional Architecture of Ice-Contact Glaciomarine Systems. *Sedimentary Geology*, 98(1-4), p. 13-43.

Lønne, I., (2001) Dynamics of marine glacier termini read from moraine architecture. *Geology*, 29(3), p. 199-202.

Lønne, I., and Nemec, W., (2011) Modes of sediment delivery to the grounding line of a fast-flowing tidewater glacier: implications for ice-margin conditions and glacier dynamics. *Ice-Marginal and Periglacial Processes and Sediments*, 354), p. 33-56.

Lønne, I., and Syvitski, J. P., (1997) Effects of the readvance of an ice margin on the seismic character of the underlying sediment. *Marine Geology*, 143(1-4), p. 81-102.

Lotter, A. F., (1985) Amsoldingersee-Late glacial and Holocene environments of a lake at the southern edge of the Swiss plateau. *Dissertation Botanicae*, 87), p. 185-208.

Matter, A., Dessolin, D., Sturm, M., and Süsstrunk, A. E., (1973) Reflexionsseismische Untersuchung des Brienzersees. *Eclogae Geologicae Helvetiae*, 66), p. 71-82.

Matter, A., Suesstrunk, A. E., Hinz, K., and Sturm, A., (1971) Ergebnisse reflexionsseismischer Untersuchungen im Thunersee. *Eclogae Geologicae Helvetiae*, 64(3), p. 505-520.

Meier, M. F., and Post, A., (1987) Fast Tidewater Glaciers. *Journal of Geophysical Research-Solid Earth and Planets*, 92(B9), p. 9051-9058.

Menzies, J., and Shilts, B. W., (2002), 8 - Subglacial environments. *Modern and Past Glacial Environments*, p. 183-278.

Mix, A. C., Bard, E., and Schneider, R., (2001) Environmental processes of the ice age: land, oceans, glaciers (EPILOG). *Quaternary Science Reviews*, 20(4), p. 627-657.

Monegato, G., Scardia, G., Hajdas, I., Rizzini, F., and Piccin, A., (2017) The Alpine LGM in the boreal ice-sheets game. *Scientific Reports*, 7(1), p. 2078.

Muir-Wood, R., (1989), Extraordinary Deglaciation Reverse Faulting in Northern Fennoscandia. *Earthquakes at North-Atlantic Passive Margins: Neotectonics and Postglacial Rebound*, p. 141-173.

Muir-Wood, R., (2000) Deglaciation Seismotectonics: a principal influence on intraplate seismogenesis at high latitudes. *Quaternary Science Reviews*, 19(14), p. 1399-1411.

Mullins, H. T. Eyles, N., Mullins, H. T., Hinchey, E. J., Wellner, R. W., Stephens, D. B., Anderson, J. W. T., Dwyer, T. R., and Hine, A. C., (1996), Seismic stratigraphy of the Finger Lakes: A continental record of Heinrich event H-1 and Laurentide ice sheet instability. *Subsurface geologic investigations of New York Finger Lakes: implications for late Quaternary deglaciation and environmental change*.

Ndiaye, M., Clerc, N., Gorin, G., Girardclos, S., and Fiore, J., (2014) Lake Neuchatel (Switzerland) seismic stratigraphic record points to the simultaneous Wurmian deglaciation of the Rhone Glacier and Jura Ice Cap. *Quaternary Science Reviews*, 85), p. 1-19.

Paul, F., Kaab, A., and Haeberli, W., (2007) Recent glacier changes in the Alps observed by satellite: Consequences for future monitoring strategies. *Global and Planetary Change*, 56(1-2), p. 111-122.

Penck, A., (1905) Glacial Features of the Surface of the Alps. *Geographical Teacher*, 3(2), p. 49-61.

Penck, A., and Brückner, E., (1909) Die Alpen im Eiszeitalter. Zweiter Band: Die Eiszeiten in den nördlichen Westalpen. *Leipzig: C.H. Tauschnitz*.

Piotrowski, J. A., Mickelson, D. M., Tulaczyk, S., Krzyszkowski, D., and Junge, F. W., (2001) Were deforming subglacial beds beneath past ice sheets really widespread? *Quaternary International*, 86), p. 139-150.

Preusser, F., Drescher-Schneider, R., Fiebig, M., and Schluchter, C., (2005) Re-interpretation of the Meikirch pollen record, Swiss Alpine Foreland, and implications for Middle Pleistocene chronostratigraphy. *Journal of Quaternary Science*, 20(6), p. 607-620.

Preusser, F., Reitner, J. M., and Schluchter, C., (2010) Distribution, geometry, age and origin of overdeepened valleys and basins in the Alps and their foreland. *Swiss Journal of Geosciences*, 103(3), p. 407-426.

Preusser, F., and Schlüchter, C., (2004) Dates from an important early Late Pleistocene ice advance in the Aare valley, Switzerland. *Eclogae Geologicae Helvetiae*, 97(2), p. 245-253.

Pugin, A., Pullan, S. E., and Sharpe, D. R., (1999) Seismic facies and regional architecture of the Oak Ridges Moraine area, southern Ontario. *Canadian Journal of Earth Sciences*, 36(3), p. 409-432.

Ravazzi, C., Pini, R., Badino, F., De Amicis, M., Londeix, L., and Reimer, P. J., (2014) The latest LGM culmination of the Garda Glacier (Italian Alps) and the onset of glacial termination. Age of glacial collapse and vegetation chronosequence. *Quaternary Science Reviews*, 105), p. 26-47.

Reber, R., Akçar, N., Ivy-Ochs, S., Tikhomirov, D., Burkhalter, R., Zahno, C., Lüthold, A., Kubik, P. W., Vockenhuber, C., and Schlüchter, C., (2014) Timing of retreat of the Reuss Glacier (Switzerland) at the end of the Last Glacial Maximum. *Swiss Journal of Geosciences*, 107(2), p. 293-307.

Reber, R., and Schlunegger, F., (2016) Unravelling the moisture sources of the Alpine glaciers using tunnel valleys as constraints. *Terra Nova*, 28(3), p. 202-211.

Reimer, P. J., Bard, E., Bayliss, A., Beck, J. W., Blackwell, P. G., Ramsey, C. B., Buck, C. E., Cheng, H., Edwards, R. L., Friedrich, M., Grootes, P. M., Guilderson, T. P., Haflidason, H., Hajdas, I., Hatte, C., Heaton, T. J., Hoffmann, D. L., Hogg, A. G., Hughen, K. A., Kaiser, K. F., Kromer, B., Manning, S. W., Niu, M., Reimer, R. W., Richards, D. A., Scott, E. M., Southon, J. R., Staff, R. A., Turney, C. S. M., and van der Plicht, J., (2013) Intcal13 and Marine13 Radiocarbon Age Calibration Curves 0-50,000 Years Cal Bp. *Radiocarbon*, 55(4), p. 1869-1887.

Reitner, M., Jürgen, Ivy-Ochs, S., Drescher-Schneider, R., Hajdas, I., and Linner, M., (2016) Reconsidering the current stratigraphy of the Alpine Lateglacial: Implications of the sedimentary and morphological record of the Lienz area (Tyrol/Austria). *Quaternary Science Journal*, 65(2.

Schlüchter, C., (1979) Übertiefte Talabschnitte im Berner Mittelland. *Eiszeitalter und Gegenwart*, 29), p. 101-113.

Schlüchter, C., (1988) The deglaciation of the Swiss-Alps: A paleoclimatic event with chronological problems. *Bulletin de l'Association francaise pour l'étude du Quaternaire*, 25(2), p. 141-145.

Schlüchter, C., (1989a) The Most Complete Quaternary Record of the Swiss Alpine Foreland. *Palaeogeography Palaeoclimatology Palaeoecology*, 72(1-2), p. 141-146.

Schlüchter, C., (1989b) Thalgut - a Comprehensive Quaternary Record of the Northern Swiss Alpine Foreland. *Eclogae Geologicae Helvetiae*, 82(1), p. 277-284.

Schlüchter, C., and Kelly, M., (2000) Das Eiszeitalter in der Schweiz. Eine schematische Zusammenfassung. *Stiftung Landschaft und Kies*, IGCP-378), p. 4.

Schnellmann, M., Anselmetti, F. S., Giardini, D., and McKenzie, J. A., (2006) 15,000 Years of mass-movement history in Lake Lucerne: Implications for seismic and tsunami hazards. *Eclogae Geologicae Helvetiae*, 99(3), p. 409-428.

van Rensbergen, P., de Batist, M., Beck, C., and Chapron, E., (1999) High-resolution seismic stratigraphy of glacial to interglacial fill of a deep glacigenic lake: Lake Le Bourget, Northwestern Alps, France. *Sedimentary Geology*, 128(1), p. 99-129.

Van Rensbergen, P., De Batist, M., Beck, C., and Manalt, F., (1998) High-resolution seismic stratigraphy of late quaternary fill of Lake Annecy (northwestern Alps): evolution from glacial to interglacial sedimentary processes. *Sedimentary Geology*, 117(1), p. 71-96.

Verschuur, D. J., Berkhout, A. J., and Wapenaar, C. P. A., (1992) Adaptive Surface-Related Multiple Elimination. *Geophysics*, 57(9), p. 1166-1177.

Waldmann, N., Ariztegui, D., Anselmetti, F. S., Coronato, A., and Austin, J. A., (2010) Geophysical evidence of multiple glacier advances in Lago Fagnano (54 degrees S), southernmost Patagonia. *Quaternary Science Reviews*, 29(9-10), p. 1188-1200.

Welten, M., (1988) Neue pollenanalytische Ergebnisse über das Jüngere Quartär des nordlichen Alpenvorlandes der Schweiz (Mittel-und Jungpleistozän). *Beiträge zur Geologischen Karte der Schweiz,* 162), p. 52.

Widess, M. B., (1973) How Thin Is a Thin Bed. *Geophysics*, 38(6), p. 1176-1180.

Wirsig, C., Zasadni, J., Ivy-Ochs, S., Christl, M., Kober, F., and Schlüchter, C., (2016) A deglaciation model of the Oberhasli, Switzerland. *Journal of Quaternary Science*, 31(1), p. 46-59.

Wirth, S. B., Girardclos, S., Rellstab, C., and Anselmetti, F. S., (2011) The sedimentary response to a pioneer geo-engineering project: Tracking the Kander River deviation in the sediments of Lake Thun (Switzerland). *Sedimentology*, 58(7), p. 1737-1761.

Wissing, S. B., and Pfiffner, O. A., (2002) Structure of the eastern Klippen nappe (BE, FR): Implications for its Alpine tectonic evolution. *Eclogae Geologicae Helvetiae*, 95(3), p. 381-398.

Wong, G. S. K., and Zhu, S. M., (1995) Speed of Sound in Seawater as a Function of Salinity, Temperature, and Pressure. *Journal of the Acoustical Society of America*, 97(3), p. 1732-1736.